

# 000 001 002 003 004 005 006 007 008 009 010 011 012 013 014 015 016 017 018 019 020 021 022 023 024 025 026 027 028 029 030 031 032 033 034 035 036 037 038 039 040 041 042 043 044 045 046 047 048 049 050 051 052 053 THE PRICE OF ROBUSTNESS: STABLE CLASSIFIERS NEED OVERPARAMETERIZATION

Anonymous authors

Paper under double-blind review

## ABSTRACT

The relationship between overparameterization, stability, and generalization remains incompletely understood in the setting of discontinuous classifiers. We address this gap by establishing a generalization bound for finite function classes that improves inversely with *class stability*, defined as the expected distance to the decision boundary in the input domain (margin). Interpreting class stability as a quantifiable notion of robustness, we derive as a corollary a *law of robustness for classification* that extends the results of Bubeck and Sellke beyond smoothness assumptions to discontinuous functions. In particular, any interpolating model with  $p \approx n$  parameters on  $n$  data points must be *unstable*, implying that substantial overparameterization is necessary to achieve high stability. We obtain analogous results for (parameterized) infinite function classes by analyzing a stronger robustness measure derived from the margin in the codomain, which we refer to as the *normalized co-stability*. Experiments support our theory: stability increases with model size and correlates with test performance, while traditional norm-based measures remain largely uninformative.

## 1 INTRODUCTION

The generalization behavior of overparameterized neural networks presents fundamental challenges to classical statistical learning theory. Traditional complexity measures, such as parameter counts or spectral norms of weights, form the basis of many generalization bounds, including those derived from VC dimension theory (Sain, 1996) and Rademacher complexity (Bartlett & Mendelson, 2002). However, these approaches do not adequately explain several empirical phenomena, e.g., *double descent* (Belkin et al., 2019) and *benign overfitting* (Bartlett et al., 2020). The occurrence of double descent illustrates that the test error, after initially increasing near the interpolation threshold, can improve as the model size continues to grow. Similarly, the phenomenon of benign overfitting demonstrates that models that perfectly interpolate noisy training data can nonetheless achieve strong generalization. Such findings expose the limitations of norm- and size-based complexity measures as predictors of generalization.

A large-scale empirical study evaluating more than forty complexity measures found that many norm-based quantities not only fail to correlate with generalization, but often even correlate negatively (Jiang et al., 2019). Beyond optimization-related metrics, one of the few quantities that consistently correlated with generalization was the margin, i.e., the distance to the decision boundary, closely related to the notion of (co-)stability we develop in this work. This aligns with an emerging perspective: generalization in modern networks is governed less by model size or norms, and more by the *stability / robustness* of predictions under input perturbations (Soloff et al., 2025; Ghosh & Belkin, 2023; Zhang et al., 2022). Related insights also arise from the literature on algorithmic stability (Bousquet & Elisseeff, 2002) and flat minima (Keskar et al., 2017). However, most theoretical results in this direction are restricted to linear models.

An exception is the *universal law of robustness* of Bubeck & Sellke (2021), which, under mild distributional assumptions, establishes a formal link between robustness, generalization, and overparameterization: smoothness and overparameterization need to balance in order to ensure good generalization while overfitting. The *law of robustness* relies on the assumption that the function class is Lipschitz, which makes it inadequate for classifiers whose codomain is discrete by design. We therefore take a step toward the open challenge posed in Bubeck & Sellke (2021, p. 4): “[...]

054 it is an interesting challenge to understand for which notions of smoothness there is a tradeoff with  
 055 size.” Specifically, we introduce *class stability* and *normalized co-stability* as geometric smooth-  
 056 ness measures that extend robustness laws to classification. In fact, replacing Lipschitz continuity  
 057 is essential: simply focusing on the Lipschitz constant of an underlying score function  $g$ , where the  
 058 classifier is of type  $f := \arg \max \circ g$ , is not informative. In particular, since  $g$  can be arbitrarily  
 059 rescaled without changing the predictions of  $f$ , its Lipschitz constant does not need to reflect the  
 060 geometry of the decision boundary (Liu & Hansen, 2024).

061  
 062 **Paper Roadmap.** We discuss related work in Section 2. Section 3 introduces class stability and  
 063 the isoperimetry assumption, a concentration property of the data that underlies our analysis. Sec-  
 064 tion 4 presents a generalization bound for finite hypothesis classes and examines its implications  
 065 for overparameterization. In Section 5, we extend the framework to infinite function classes via the  
 066 notion of normalized co-stability. Our theoretical predictions are tested experimentally on MNIST  
 067 and CIFAR-10 in Section 6. Finally, Section 7 concludes with a discussion of open directions.

068 **Contributions.** We provide a summary of our main results.  
 069

070 1) We prove that, under an isoperimetry assumption on the data distribution, the data-dependent  
 071 Rademacher complexity of a finite hypothesis class of classifiers can be bounded in terms of the  
 072 minimum *class stability*. This yields an improved generalization bound for discontinuous classifiers  
 073 (Theorem 4), which tightens as stability increases.  
 074  
 2) We show that in the classically parameterized regime ( $\#\text{parameters} \approx \#\text{samples}$ ), any interpolating  
 075 classifier must be unstable (Corollary 6) with high probability. Consequently, achieving both near-  
 076 perfect fitting and high class stability requires substantial overparameterization of order  $p \approx nd$ .  
 077  
 3) We extend the framework to infinite function classes by considering classifiers of the form  
 078  $f(x) := \arg \max \circ g_w(x)$ , where  $g_w$  is a parameterized Lipschitz-continuous (in both  $x$  and  $w$ )  
 079 score function. This enables us to define a robustness measure – the *normalized co-stability* –, based  
 080 on output score margins, and derive a corresponding generalization bound (Theorem 13). The added  
 081 regularity also results in a law of robustness for infinite function classes (Corollary 15).  
 082  
 4) We empirically validate our predictions on MNIST and CIFAR-10, observing that stability and  
 083 normalized co-stability grow with network width and closely track test error, supporting our claim  
 084 that generalization in overparameterized regimes is driven by (normalized co-)stability.  
 085

086 Taken together, our results extend the law of robustness to discontinuous classifiers and highlight  
 087 stability as a central factor in understanding generalization in modern networks.

## 089 2 RELATED WORK

091 **Smoothness-based generalization.** Our work is inspired by the *law of robustness* of Bubeck &  
 092 Sellke (2021), which shows that regression with Lipschitz predictors generalizes when smoothness  
 093 and overparameterization are properly balanced. Subsequent works have extended this perspective:  
 094 for example, Zhu et al. (2023) investigate how width, depth, and initialization affect robustness,  
 095 while more recent studies Das et al. (2025) establish refined smoothness–generalization trade-offs  
 096 for a wider range of loss landscapes.

097 **Margin-based generalization.** Classical generalization bounds combine a margin term, defined  
 098 with respect to a score function, with a capacity measure – for example, spectrally-normalized mar-  
 099 gin bounds (Bartlett et al., 2017) or path-norm bounds (Neyshabur et al., 2018). Recent extensions  
 100 include multi-class margin bounds in terms of margin-normalized geometric complexity (Munn  
 101 et al., 2024). These approaches are closely aligned with our normalized co-stability perspective:  
 102 both control a codomain margin while coupling it to a regularity property of the score function, and  
 103 both recover inverse-margin scaling.

105 Input-space margin bounds have also been studied, yielding that generalization is controlled by the  
 106 minimum robustness radius (Sokolic et al., 2017), while sample-complexity lower bounds show that  
 107 adversarial robustness increases the VC dimension (Gao et al., 2019). Our notion of *class stability*  
 differs: it is the *expected input margin* – the average distance to the decision boundary under the

108 data distribution – rather than a minimum or an empirical quantile. This measure is closely tied to  
 109 robustness (Fawzi et al., 2016; Gilmer et al., 2018) and induces data-dependent bounds that track  
 110 generalization.  
 111

112 **Limits of uniform generalization bounds.** Uniform convergence-based bounds are often vacuous  
 113 in overparameterized networks (Nagarajan & Kolter, 2021), since SGD appears to find solutions  
 114 at a macroscopic level (supporting generalization) but with microscopic fluctuations that break uniform  
 115 analyses. Our bounds remain uniform but depend on macroscopic, distribution-dependent  
 116 quantities: the Rademacher complexity—our applied technique to derive generalization bounds—  
 117 is controlled by stability (or co-stability). Whether this structure avoids the vacuity identified by  
 118 Nagarajan & Kolter (2021) remains open.  
 119

120 **Stability, robustness, and implicit bias.** Algorithmic stability (Bousquet & Elisseeff, 2002) and  
 121 the flat minima literature (Keskar et al., 2017) argue that robustness under perturbations drives  
 122 generalization. More recently, Zou et al. (2024) derive out-of-distribution generalization bounds based  
 123 on the sharpness of the learned minima. Our contribution is to extend a stability-based perspective  
 124 to discontinuous neural classifiers, both theoretically and empirically. Complementary work on im-  
 125 plicit bias shows that gradient descent favors solutions with a small number of connected decision  
 126 regions, a proxy for large input-space margin (Li et al., 2025). This suggests that optimization dy-  
 127 namics may implicitly favor the same geometric simplicity that our stability-based bounds capture.  
 128

129  
 130 **Out-of-Distribution Generalization.** Classically and also in our analysis, generalization is based  
 131 on the independently and identically distributed assumption on the data, in particular, the test data are  
 132 generated from the same distribution as the training data coined In-Distribution (ID) generalization.  
 133 In contrast, Out-of-Distribution (OOD) generalization aims to study the generalization performance  
 134 under distributional shifts. To make the problem tractable the potential shifts are constrained to, for  
 135 instance, spurious correlations or covariate shifts. In the OOD setting the connection between over-  
 136 parameterization and generalization has been studied in a series of theoretical works with positive  
 137 Hao et al. (2024) and negative results Sagawa et al. (2020); Wald et al. (2024).  
 138

139 Adversarial robustness can be viewed as a special case of OOD generalization, where the distri-  
 140 butional shift is constrained to lie within a perturbation set Sinha et al. (2020). In this sense, our  
 141 stability-based analysis is conceptually connected to OOD generalization. However, our results do  
 142 not provide explicit bounds on OOD error; instead, we focus on ID generalization under the as-  
 143 sumption that the classifier satisfies a given level of adversarial robustness expressed as the margin.  
 144

### 3 PRELIMINARIES AND NOTATION

145 In the following, we provide background on the key concepts underlying our analysis, namely sta-  
 146 bility, generalization, and isoperimetry. For clarity of exposition, we present our results in the binary  
 147 classification setting. The extension to multi-class problems follows by a one-vs-all reduction; see  
 148 Appendix F for details. Thus, let  $(\mathcal{X} \times \{-1, 1\}, \mu)$  be a probability measure space with  $\mathcal{X} \subset \mathbb{R}^d$   
 149 bounded and  $\mathcal{F} \subset \{f \mid f : \mathcal{X} \rightarrow \{-1, 1\}\}$  a set of classifiers. The goal is to find a stable function  
 150  $f \in \mathcal{F}$  minimizing a bounded loss function  $\ell : \{-1, 1\}^2 \rightarrow \mathbb{R}_+$  on  $n$  i.i.d. samples  $(x_i, y_i) \sim \mu$ . A  
 151 natural loss in the classification setting is the 0-1 loss  $\ell_{0-1}(y, y') := \mathbb{1}_{y \neq y'}$ . In this setup, following  
 152 a similar approach as in Liu & Hansen (2024), we define the *class stability* of  $f$  as the expected  
 153 distance of a sample to the decision boundary in  $\mathcal{X}$ , thereby capturing the average robustness of a  
 154 classifier  $f$  to input perturbations.  
 155

156 **Definition 1** (Margin and Class Stability). *Let  $f : \mathcal{X} \rightarrow \{-1, 1\}$ . The signed distance function  $d_f$   
 157 of  $f$  at  $x \in \mathcal{X}$  is defined as*  
 158

$$d_f(x) := \begin{cases} d(x, f^{-1}(\{-1\})), & \text{if } f(x) = 1, \\ -d(x, f^{-1}(\{1\})), & \text{if } f(x) = -1, \end{cases}$$

162 where  $d(x, A) := \inf_{y \in A} \|x - y\|_2$ . We define the (unsigned) margin  $h_f$  at  $x$  as the absolute value  
 163 of the signed distance function,  
 164

$$165 \quad h_f(x) := |d_f(x)| = \inf\{\|x - z\|_2 : f(z) \neq f(x), z \in \mathbb{R}^d\}.$$

166 The class stability  $S(f)$  of  $f$  is its expected margin under the data distribution:

$$167 \quad S(f) := \mathbb{E}[h_f].$$

168 **Remark 2.** The signed distance function  $d_f$  is 1-Lipschitz if  $\mathcal{X}$  is path-connected. Moreover, if  
 169  $\text{sgn}(0) = 1$  and  $f^{-1}(\{1\})$  is closed in  $\mathcal{X}$ , then  $f$  admits the representation  $f = \text{sgn} \circ d_f$  (see  
 170 Appendix B for details).  
 171

172 Our goal is to relate the class stability to the Rademacher complexity of a function class, which,  
 173 in turn, connects to *generalization* bounds through classical results (Bartlett & Mendelson, 2002).  
 174 In particular, for a bounded loss  $|\ell| \leq a$ , the difference between the *population risk*  $R_\ell(f) :=$   
 175  $\mathbb{E}[\ell(f(x), y)]$  and the *empirical risk*  $\hat{R}_\ell(f) := \frac{1}{n} \sum_{i=1}^n \ell(f(x_i), y_i)$  is bounded with probability at  
 176 least  $1 - \delta$  over the samples by

$$177 \quad \sup_{f \in \mathcal{F}} (R_\ell(f) - \hat{R}_\ell(f)) \leq 2\mathcal{R}_{n,\mu}(\ell \circ \mathcal{F}) + a\sqrt{\frac{2\log(2/\delta)}{n}}, \quad (1)$$

180 where  $\mathcal{R}_{n,\mu}(\mathcal{G})$  denotes the *Rademacher complexity* of a general function class  $\mathcal{G}$ , defined as  
 181

$$182 \quad \mathcal{R}_{n,\mu}(\mathcal{G}) = \frac{1}{n} \mathbb{E}^{\sigma_i, x_i} \left[ \sup_{g \in \mathcal{G}} \left| \sum_{i=1}^n \sigma_i g(x_i) \right| \right],$$

184 with  $(\sigma_i)_{i=1}^n$  i.i.d. Rademacher random variables. To obtain a bound in Equation 1 in terms of  
 185  $\mathcal{R}_{n,\mu}(\mathcal{F})$ , note that  $\mathcal{R}_{n,\mu}(\ell \circ \mathcal{F}) \leq C\mathcal{R}_{n,\mu}(\mathcal{F})$  holds under certain conditions on the loss, we have  
 186

$$187 \quad \mathcal{R}_{n,\mu}(\ell_{0-1} \circ \mathcal{F}) \leq \frac{1}{2} \mathcal{R}_{n,\mu}(\mathcal{F}), \quad \text{i.e., } C = \frac{1}{2}, \quad (2)$$

189 whereas for  $L$ -Lipschitz losses  $C = L$  holds, see Bartlett & Mendelson (2002); Shalev-Shwartz  
 190 & Ben-David (2014) for detailed explanations. Overall, it therefore suffices to bound  $\mathcal{R}_{n,\mu}(\mathcal{F})$  in  
 191 terms of the class stability of functions  $f \in \mathcal{F}$  in order to link generalization to stability. Equiv-  
 192 alently, the key step is to control how well stable functions can fit random labels, which requires  
 193 structural assumptions on the input distribution. We discuss in detail in Appendix A why such as-  
 194 sumptions are unavoidable. A natural and widely used condition is *isoperimetry*, which guarantees  
 195 sharp concentration for bounded Lipschitz-continuous functions (Bubeck & Sellke, 2021).

196 **Definition 3** (Isoperimetry). A probability measure  $\mu$  on  $\mathcal{X} \subset \mathbb{R}^d$  satisfies  $c$ -isoperimetry if for any  
 197 bounded  $L$ -Lipschitz function  $f : \mathcal{X} \rightarrow \mathbb{R}$ , and any  $t \geq 0$ ,

$$198 \quad \mathbb{P}(|f(x) - \mathbb{E}[f]| \geq t) \leq 2e^{-\frac{dt^2}{2cL^2}}. \quad (3)$$

200 Isoperimetry is, for instance, satisfied by Gaussian measures and the volume measure on Riemannian  
 201 manifolds with positive curvature, such as the uniform measure on the sphere (Vershynin, 2018;  
 202 Bubeck & Sellke, 2021). Consequently, under the manifold hypothesis, the relevant dimension in  
 203 our bounds can be interpreted as the intrinsic manifold dimension rather than the ambient dimension.  
 204

## 205 4 A LAW OF ROBUSTNESS FOR CLASSIFICATION

207 In this section, we establish a *law of robustness for classification*, extending stability-generalization  
 208 trade-offs to discontinuous functions. Classical results for smooth functions characterize robustness  
 209 via the Lipschitz constant, which is ill-defined for classifiers with discrete outputs. To address this,  
 210 we follow the general strategy of Bubeck & Sellke (2021) (see Appendix A for details), but replace  
 211 their use of Lipschitz continuity with our notion of *class stability* (Definition 1). Formally, we  
 212 proceed under the following assumptions:

213 (H1)  $(\mathcal{X} \times \{-1, 1\}, \mu)$  is a probability space with bounded sample space  $\mathcal{X}$  and  $c$ -isoperimetric<sup>1</sup>  
 214 marginal distribution  $\mu_{\mathcal{X}}$ ;

215 <sup>1</sup>It is worth noting that our framework can be readily extended to mixtures of  $c$ -isoperimetric distributions.

216 (H2) the considered hypothesis class  $\mathcal{F}$  of classifiers  $f : \mathcal{X} \rightarrow \{-1, 1\}$  is finite, that is  $|\mathcal{F}| < \infty$ .  
 217

218 These conditions ensure concentration of measure in the input space and allow complexity control  
 219 via a union bound. With this structure in place, class stability can be related to the Rademacher  
 220 complexity, leading to the bound stated below.

221 **Theorem 4** (Rademacher Bound). *Suppose Assumptions (H1) and (H2) hold, and that  
 222  $\min_{f \in \mathcal{F}} S(f) > S > 0$  with  $\log |\mathcal{F}| \geq n$ .*

224 1. *The Rademacher complexity satisfies*

$$226 \quad \mathcal{R}_{n,\mu}(\mathcal{F}) \leq K_1 \max \left\{ \frac{1}{\sqrt{n}}, \frac{\sqrt{c}}{S} \cdot \frac{\log |\mathcal{F}|}{n\sqrt{d}} \right\}, \quad (4)$$

228 for an absolute constant  $K_1 > 0$ .

230 2. *If, in addition,  $f^{-1}(\{1\})$  is closed and  $\mathcal{X}$  path-connected, the bound sharpens to*

$$232 \quad \mathcal{R}_{n,\mu}(\mathcal{F}) \leq K_2 \max \left\{ \frac{1}{\sqrt{n}}, \frac{\sqrt{c}}{S} \sqrt{\frac{\log |\mathcal{F}|}{nd}}, 2 \exp \left( - \frac{dS^2}{8c} \right) \right\}, \quad (5)$$

235 for another absolute constant  $K_2 > 0$ .

237 *Proof sketch.* Equation 4 is obtained via a Lipschitz surrogate argument combined with isoperimetry. The refined bound in Equation 5 further leverages the representation  $f = \text{sgn} \circ d_f$  (Remark 2),  
 238 using that large stability ensures  $d_f$  remains well separated from the discontinuity at 0. Complete  
 239 details are provided in Appendix C.  $\square$

242 **Remark 5.** *In contrast to Bubeck & Sellke (2021), where stability is measured by the minimal  
 243 Lipschitz constant of the function class, our initial bound in Theorem 4 incurred an additional factor  
 244  $\sqrt{\log |\mathcal{F}|/n}$  in the regime  $\log |\mathcal{F}| \geq n$ . By assuming mild regularity conditions, we can eliminate  
 245 this gap and recover the same scaling as in Bubeck & Sellke (2021).*

246 The key insight of Theorem 4, combined with the classical generalization bound in Equation 1, is  
 247 that *good generalization* can still be achieved in the highly *overparameterized* regime—provided the  
 248 classifiers exhibit sufficiently *high class stability*. Indeed, the presence of  $\frac{1}{S}$  in front of  $\sqrt{\log |\mathcal{F}|}$  in  
 249 Equation 4 and Equation 5 indicates that class stability affects the effective complexity of the model  
 250 class, potentially mitigating the risks of overfitting in large models. Note that, using a uniform  
 251 discretization, a finite approximation of an infinite function class parameterized with  $p$  parameters  
 252 over a bounded subset of  $\mathbb{R}^p$  satisfies  $\log |\mathcal{F}| \in \mathcal{O}(p)$ . In this sense,  $\log |\mathcal{F}|$  reflects the number of  
 253 model parameters. Therefore, when the number of parameters  $p \approx \log |\mathcal{F}|$  is much larger than  $n$ ,  
 254 the second term in the maximum in Equation 5 dominate, and the bounds becomes small if  $S$  scales  
 255 at least in the order of  $\sqrt{\frac{p}{nd}}$ .

256 We are now ready to state our *law of robustness for discontinuous functions*, obtained as a direct  
 257 corollary of the refined Rademacher bound in Equation 5 of Theorem 4.

259 **Corollary 6** (Law of Robustness for Discontinuous Functions). *Assume (H1), (H2), and the addi-  
 260 tional conditions in 2. of Theorem 4 hold. Let  $p := \log |\mathcal{F}| \geq n$ . Fix  $\varepsilon, \delta \in (0, 1)$  and consider the  
 261 0–1 loss  $\ell_{0-1}$ . There exists an absolute constant  $K > 0$  such that, if*

262 1. *the minimal risk  $\sigma^2 := \min_{f \in \mathcal{F}} R_{0-1}(f)$  satisfies  $\sigma^2 \geq \varepsilon$ , and*

264 2. *the sample size  $n$  is large enough to ensure (i)  $\frac{K}{\sqrt{n}} < \frac{\varepsilon}{3}$  and (ii)  $\sqrt{\frac{2 \log(2/\delta)}{n}} < \frac{\varepsilon}{2}$ ,*

266 then with probability at least  $1 - \delta$  (over the sample), the following holds uniformly for all  $f \in \mathcal{F}$ :

$$268 \quad \hat{R}_{0-1}(f) \leq \sigma^2 - \varepsilon \implies S(f) < \max \left\{ \frac{3K}{\varepsilon} \sqrt{\frac{c \log |\mathcal{F}|}{nd}}, \sqrt{\frac{8c}{d} \log \left( \frac{6K}{\varepsilon} \right)} \right\}. \quad (6)$$

270 *Proof sketch.* Apply the Rademacher bound (Theorem 4) to the high-stability subset  $\mathcal{F}_{S_*} := \{f \in \mathcal{F} : S(f) \geq S_*\}$ . For  $S_*$  chosen large enough, such functions cannot achieve empirical risk below 271  $\sigma^2 - \varepsilon$ , so any interpolating classifier with risk  $\leq \sigma^2 - \varepsilon$  must lie outside  $\mathcal{F}_{S_*}$ , i.e., must satisfy 272  $S(f) < S_*$ . The full proof is provided in Appendix D.  $\square$

273 **Remark 7.** Unlike Bubeck & Sellke (2021), which assume Lipschitz-continuous losses, our analysis 274 directly addresses the discontinuous 0–1 loss, making it more natural for classification tasks. The 275 overall proof strategy, however, extends to arbitrary losses provided one can derive an appropriate 276 bound on the Rademacher complexity of the composed function class, as in Equation 2.

277 **Remark 8.** Importantly, this result also covers intrinsically discontinuous classifiers, such as quantized 278 neural networks and spiking neural networks. Moreover, since self-attention is in general not 279 Lipschitz-continuous Kim et al. (2021), our framework appears particularly well-suited to the 280 analysis of overparameterization of transformers, which underlie most state-of-the-art language 281 models.

282 From Equation 6 we conclude that achieving both low training error and high stability requires 283 parameterization on the order  $p \approx nd$ . This necessity arises in the high-dimensional regime, since 284 when  $d$  is large the first term in the maximum dominates for  $p \geq n$ . This reinforces our central 285 message: overparameterization may not harm generalization, but on the contrary, is necessary for 286 achieving robustness and good fitting in classification. Notably, modern neural networks, including 287 large language models (LLMs) (Brown et al., 2020), are trained in heavily overparameterized 288 regimes: Even though recent scaling laws Hoffmann et al. (2022) suggest a balance between model 289 and data size, these models remain functionally overparameterized in that their capacity far exceeds 290 what is required to fit the training data. Therefore, our result may help to understand why such 291 models still do generalize effectively.

## 293 5 A LAW OF ROBUSTNESS FOR INFINITE FUNCTION CLASSES

294 In Theorem 4, our analysis does not straightforwardly extend to infinite function classes. The usual 295 proof strategy via a covering-number argument requires closeness in parameter space to imply close- 296 ness in function space. In Bubeck & Sellke (2021), this is enforced via Lipschitz continuity in the 297 parameters of the function class, but such a condition is in general meaningless for discontinuous 298 classifiers.

299 To overcome this, we restrict our attention to function classes with additional structure and introduce 300 a strengthened stability notion. Specifically, we impose a representation analogous to Remark 2, 301 namely,

302 (H3) The hypothesis class has the form  $\mathcal{F} = \text{sgn} \circ \mathcal{G}$ , where  $\mathcal{G} = \{g_w : \mathcal{X} \rightarrow [-1, 1] : w \in \mathcal{W}\}$  303 is a parameterized family of Lipschitz functions. The parameter space  $\mathcal{W} \subset \mathbb{R}^p$  is bounded 304 with  $\text{diam}(\mathcal{W}) \leq W$ , and the parameterization is Lipschitz:

$$308 \quad \|g_{w_1} - g_{w_2}\|_\infty \leq J \|w_1 - w_2\|.$$

310 The extension from finite to infinite classes requires not only (i) Lipschitz continuity in  $w$ , but also 311 (ii) that the scores  $g_w(x)$  stay quantitatively away from zero, so that small parameter perturbations 312 cannot cause arbitrary label flips. Class stability alone does not suffice to ensure (ii), as the following 313 example demonstrates.

314 **Example 9** (Class stability does not prevent discontinuity). Let  $\mathcal{G} = \{g_w(x) = w \tanh(x) : w \in 315 [-1, 1]\}$ . The parameterization is Lipschitz since

$$316 \quad \|g_{w_1} - g_{w_2}\| \leq \|w_1 - w_2\|.$$

317 For  $w_1 = \frac{\varepsilon}{2}$  and  $w_2 = -w_1$ ,  $\|w_1 - w_2\| \leq \varepsilon$ , yet

$$319 \quad \|\text{sgn}(g_{w_1}(x)) - \text{sgn}(g_{w_2}(x))\| = 2$$

320 for almost all  $x$ . Each classifier has a single boundary (hence high class stability), but parameter 321 proximity does not imply classifier proximity.

322

323 To guarantee property (ii), we introduce a new robustness measure in the codomain.

324 **Definition 10** (Co-margin and Co-stability). Let  $f = \text{sgn} \circ g : \mathcal{X} \rightarrow \{-1, 1\}$ . The co-margin at  $x$  is

$$325 \quad 326 \quad 327 \quad h_g^*(x) := |g(x)|,$$

328 and we denote the normalized co-margin as

$$329 \quad 330 \quad \bar{h}_g^*(x) := \frac{|g(x)|}{L(g)},$$

331 where  $L(g)$  is the Lipschitz constant of  $g$ . The co-stability is then the expected co-margin

$$332 \quad 333 \quad S^*(g) := \mathbb{E}[h_g^*(x)],$$

334 and the normalized co-stability is accordingly defined as the expected normalized co-margin

$$335 \quad \bar{S}^*(g) := \mathbb{E}[\bar{h}_g^*(x)].$$

336 **Remark 11** (Representation dependence). Unlike class stability  $S(f)$ , which depends only on the  
337 decision boundary of  $f$ , the co-stability  $S^*(g)$  and its normalized form  $\bar{S}^*(g)$  depend on the particular  
338 representation  $f = \text{sgn} \circ g$ . Different score functions  $g$  inducing the same classifier  $f$  can yield  
339 different values of  $S^*(g)$  and  $\bar{S}^*(g)$ . For the specific representation  $f = \text{sgn} \circ d_f$  from Lemma 18,  
340 however, the quantities coincide:  $S^*(g) = \bar{S}^*(g) = S(f)$ .

341 Imposing  $S^*(g) \geq S^* > 0$  ensures that scores remain, on average, a non-trivial distance away from  
342 zero. Together with (H3), co-stability provides the continuity and separation properties required for  
343 infinite-class generalization bounds.

344 Before turning to the formal statement of this fact, we want to discuss the relation of class stability  
345 and co-stability. The connection between input- and codomain-based margins is immediate since

$$346 \quad 347 \quad 348 \quad h_g(x) \geq \frac{h_g^*(x)}{L(g)} = \bar{h}_g^*(x).$$

349 By  $L(g)$ -Lipschitz continuity, moving  $x$  by  $r$  changes  $g(x)$  by at most  $L(g)r$ , so flipping the prediction  
350 requires  $r \geq |g(x)|/L(g)$ . Taking expectations yields

$$351 \quad S(f) \geq \bar{S}^*(g). \quad (7)$$

352 Thus normalized co-stability lower-bounds class stability. This inequality highlights two levers for  
353 improving generalization: increasing  $S^*(g)$  or decreasing  $L(g)$ . Importantly,  $\bar{S}^*(g)$ , like  $S(f)$ , is  
354 invariant to input rescaling and therefore serves as a natural robustness measure.

355 **Remark 12.** A related ratio,  $\frac{\gamma}{\mathcal{R}_f}$ , appears in Bartlett et al. (2017), where  $\gamma$  is the minimum margin  
356 and  $\mathcal{R}_f$  a spectral complexity term controlling Lipschitzness. Empirically, Lipschitz margin training,  
357 which enforces

$$358 \quad \bar{S}^*(g) \geq c,$$

359 improves adversarial robustness (Tsuzuku et al., 2018). Moreover, Béthune et al. (2022, Corollary 2)  
360 show that among maximally accurate classifiers, there exists a 1-Lipschitz solution that achieves  
361 maximal co-margins and satisfies  $S(f) = S^*(g)$ . In particular, the Bayes classifier admits the  
362 representation  $b = \text{sgn} \circ d_b$ , which fulfills these properties.

363 Combining Theorem 4 with Equation 7, the Rademacher complexity of a finite function class  $\mathcal{F} =$   
364  $\text{sgn} \circ \mathcal{G}$  can be bounded in terms of normalized co-stability as

$$365 \quad 366 \quad 367 \quad \mathcal{R}_{n,\mu}(\mathcal{F}) \leq K_2 \max \left\{ \frac{1}{\sqrt{n}}, \sqrt{c} \frac{L}{S^*} \sqrt{\frac{\log |\mathcal{F}|}{nd}}, 2 \exp \left( - \frac{dS^{*2}}{L^2 8c} \right) \right\},$$

368 where  $S^* > 0$  and  $L > 0$  are bounds on the minimal co-stability and maximal Lipschitz constant,  
369 respectively. Under condition (H3), the statement can be extended to infinite function classes.

370 **Theorem 13.** Suppose (H1) and (H3) hold, and that  $S^*(g) > S^* > 0$  and  $L(g) \leq L$  for all  $g \in \mathcal{G}$ .  
371 Assume further that  $p \geq n$ . Then, for any covering precision  $\tilde{\varepsilon} > 0$ ,

$$372 \quad 373 \quad 374 \quad \mathcal{R}_{n,\mu}(\mathcal{F}) \leq K \max \left\{ \sqrt{\frac{1}{n}}, \frac{L}{S^*} \sqrt{\frac{p}{nd}} \sqrt{c \log(1 + 60WJ\tilde{\varepsilon}^{-1})}, 2 \exp \left( - \frac{dS^{*2}}{8cL^2} \right), \frac{J}{S^*} \tilde{\varepsilon} \right\}, \quad (8)$$

375 where  $K > 0$  is an absolute constant independent of  $p, n, d, S^*, c, L, J, \tilde{\varepsilon}, W$ .

378 *Proof sketch.* The proof follows the previously mentioned  $\varepsilon$ -net approach, standard in infinite-class  
 379 settings. The Lipschitz continuity in  $w$  (from (H3)) controls the covering number of  $\mathcal{G}$  at scale  $\tilde{\varepsilon}$ ,  
 380 while co-stability ensures that small perturbations in  $w$  do not induce flips through the sgn mapping.  
 381 The additional term  $\frac{J}{S^*} \tilde{\varepsilon}$  reflects the residual error introduced by the discretization. See Appendix E  
 382 for more details.  $\square$

384 **Remark 14.** The factor  $\frac{L}{S^*}$  shows that generalization depends jointly on the average prediction  
 385 confidence  $S^*(g)$  and the Lipschitz constant  $L(g)$ , the latter quantifying robustness of predicted  
 386 probabilities. This aligns with empirical findings (Khromov & Singh, 2024; Gamba et al., 2025;  
 387 Gouk et al., 2020; Sanyal et al., 2020; Béthune et al., 2022), which report that smaller Lipschitz  
 388 constants typically improve generalization, and in some cases exhibit a double-descent behavior.

389 We obtain with the same reasoning as in Corollary 6 the following law of robustness for Lipschitz-  
 390 regular infinite function classes.

391 **Corollary 15** (Law of Robustness for Infinite Function Classes). *Assume (H1) and (H3), and fix  
 392  $\varepsilon, \delta \in (0, 1)$ . Consider the 0-1 loss  $\ell_{0-1}$ . There exists an absolute constant  $K > 0$  such that, if*

394 1. *the minimal risk  $\sigma^2 := \min_{f \in \mathcal{F}} R_{0-1}(f)$  satisfies  $\sigma^2 \geq \varepsilon$ , and*

396 2. *the sample size  $n$  is large enough so that (i)  $\frac{K}{\sqrt{n}} < \frac{\varepsilon}{3}$  and (ii)  $\sqrt{\frac{2 \log(2/\delta)}{n}} < \frac{\varepsilon}{2}$ ,*

398 *then with probability at least  $1 - \delta$ , for all  $\tilde{\varepsilon} > 0$ , the following holds uniformly for all  $g \in \mathcal{G}$  and  
 399  $f_g = \text{sgn} \circ g$ :*

$$401 \hat{R}_{0-1}(f_g) \leq \sigma^2 - \varepsilon \implies \frac{S^*(g)}{L(g)} < \max \left\{ \frac{3K}{\varepsilon} \sqrt{\frac{p}{nd} \sqrt{c \log(1 + 60WJ\tilde{\varepsilon}^{-1})}}, \sqrt{\frac{8c}{d} \log \left( \frac{6K}{\varepsilon} \right)} \right\}.$$

404 **Remark 16.** As in Bubeck & Sellke (2021), we require  $W$  and  $J$  to be at most polynomial in  $(n, d, p)$   
 405 so that they do not affect the asymptotic scaling. In the case of feedforward neural networks, Bubeck  
 406 & Sellke (2021) further show that when the data distribution is concentrated in a ball of radius  $R$ ,  
 407 it suffices to assume that  $W$  is polynomially bounded.

409 Analogous to the finite-class case, we conclude that Lipschitz-regular classifiers must be over-  
 410 parameterized of order  $nd$  to achieve both low training error and high normalized co-stability. Without  
 411 sufficient parameter capacity relative to sample size and ambient dimension, robustness cannot be  
 412 guaranteed: models may fit the training data, but will necessarily exhibit either large Lipschitz con-  
 413 stants of the score function or low co-stability, reflecting weak confidence in their predictions. Thus,  
 414 overparameterization emerges as a necessary condition for robustness, not a byproduct of current  
 415 training practice, but a structural limitation dictated by geometry and probability.

## 416 6 EXPERIMENTS

419 We empirically validate our theoretical prediction that class stability  $S(f)$  and co-stability  $S(f)^*$   
 420 increase with model size in interpolating networks.

421 **Setup.** We train fully connected MLPs with four hidden layers and widths  $w \in$   
 422  $\{128, 256, 512, 1024, 2048\}$  on MNIST and up to  $w = 1024$  for CIFAR-10. All models are trained  
 423 until reaching at least 99% training accuracy, ensuring (near-)interpolation so that test accuracy  
 424 effectively coincides with generalization performance.

425 **Class Stability.** We estimate empirical class stability  $S(f)$  via adversarial perturbations. For each  
 426 input, we increase the perturbation radius  $r$  along a predefined grid  $\mathbf{r} = (r_1, \dots, r_n)$  until the  
 427 classifier's prediction changes. The minimal successful radius is recorded as the distance to the  
 428 decision boundary for that sample, and  $S(f)$  is reported as the average over the dataset.

429 **Normalized Co-Stability.** The empirical co-stability  $S^*(g)$  is computed via the multi-class margin

$$430 g_j(x) - \max_{i \neq j} g_i(x), \quad j = \arg \max_i g_i(x),$$

averaged over the dataset; see Appendix F for details about the multi-class setting. We estimate the Lipschitz constant  $L(g)$  using the efficient ECLIPSE method (Xu & Sivarajani, 2024), and report the normalized ratio  $S^*(g)/L(g)$  as a function of model size.

**Results.** Figure 1 shows that, for MLPs, both class stability  $S(f)$  and normalized co-stability  $S^*(g)/L(g)$  increase consistently with model size. The observed saturation of (normalized co-) stability aligns with theoretical intuition: the Bayes classifier admits a finite (normalized co-) stability level, and pushing beyond this level necessarily reduces accuracy - an instance of the robustness/accuracy trade-off extensively discussed in the literature (Zhang et al., 2019; Tsipras et al., 2019; Béthune et al., 2022). Accordingly, we expect stability to plateau once models approach the Bayes decision boundary. For CIFAR-10, although test accuracy remains far below the Bayes optimal (around 50%), the same reasoning applies relative to the best classifier achievable within the restricted MLP architecture.

Empirically, class stability closely tracks test accuracy, whereas standard weight norms show no systematic correlation with model size or generalization performance. On MNIST, however, we observe that normalized co-stability exhibits large seed-to-seed fluctuations and no consistent trend with model size. We conjecture that this reflects the simplicity of MNIST, which admits many local minima with highly variable score functions. To probe this hypothesis, we train 4-MLPs width widths  $w \in \{128, 256, 512, 1024\}$  using sharpness-aware optimization (SAM) (Foret et al., 2021; Kwon et al., 2021), which biases training toward flatter minima. As shown in Figure 2, this reduces variance across seeds and restores a clear monotonic dependence on model size. We note that the absolute values of stability are smaller for SAM-trained models, but this is explained by the absence of spectral normalization in SAM, which results in larger Lipschitz constants. What matters for our purposes is the monotonic trend, not the absolute scale. These findings suggest a quantitative link between sharpness and stability, and motivate further study of how optimization bias interacts with the geometric structure underlying our robustness laws.

Additional details and plots are provided in Appendix G. Moreover, our code is available here: <https://anonymous.4open.science/r/ICLR26-Stability-AC53/README.md>.

## 7 DISCUSSION AND FUTURE WORK

Our results identify class stability and its codomain analogue, normalized co-stability, as principled quantities linking overparameterization, generalization, and robustness for discontinuous classifiers. While we provide geometric laws of robustness for finite and infinite hypothesis classes, and our experiments support their validity, several directions remain open.

**Empirical directions.** Computing class stability  $S(f)$  and Lipschitz constants  $L(g)$  of neural networks is NP-hard (Katz et al., 2017; Weng et al., 2018; Scaman & Virmaux, 2019), limiting the

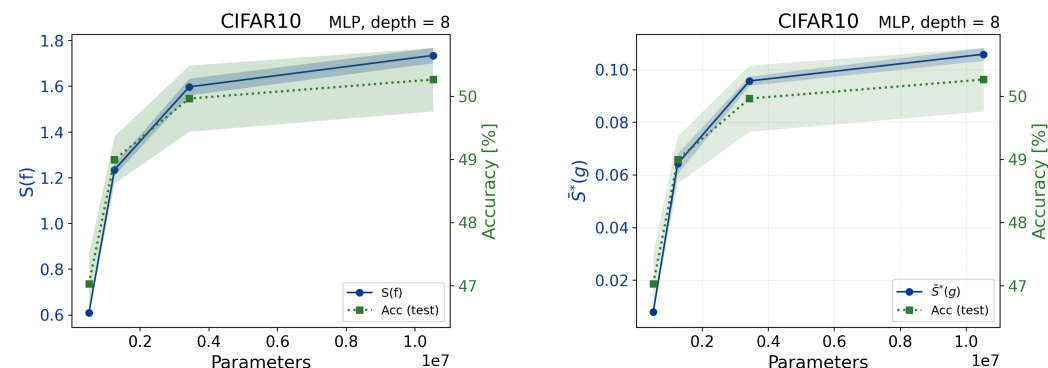


Figure 1: Stability measures for MLPs trained on CIFAR-10. Both class stability  $S(f)$  and normalized co-stability  $S^*(g) = S^*(g)/L(g)$  increase systematically with model size and closely follow test accuracy, in line with our theoretical predictions.

486 direct use of (normalized co-)stability in training. However, practical relaxations exist: normalized  
487 co-stability underlies *Lipschitz margin training* (Tsuzuku et al., 2018), while input-space stability is  
488 related to adversarial training (Madry et al., 2018; Goodfellow et al., 2015). Biasing optimization  
489 explicitly toward (co-)stable solutions is therefore a promising empirical direction. Another avenue  
490 is to probe isoperimetry and related concentration phenomena on real data. This connects to the  
491 manifold hypothesis and raises the question of whether robustness laws fail empirically when the  
492 effective dimension of the data manifold is small.

493

494 **Theoretical directions.** Our framework motivates exploring alternative geometric measures, too.  
495 Do quantities such as sharpness of the loss landscape obey robustness laws analogous to those for  
496 (normalized co-)stability? Our experiments suggest a link, calling for deeper analysis. Another  
497 question concerns sufficiency: we establish that overparameterization is necessary for generalization  
498 but is it also sufficient under suitable optimization? Bombari et al. (2023) prove sufficiency for  
499 Lipschitz regression in the NTK regime but show that it fails for a random features model. Extending  
500 such results to discontinuous classifiers may reveal qualitative differences.

501

502 Finally, the role of implicit bias remains unclear. Does gradient descent or SGD exhibit a bias toward  
503 classifiers with higher (normalized co-)stability, as suggested by analogous results on region counts  
(Li et al., 2025)? Establishing such a bias would explain why stable solutions emerge in practice.

504

505 Overall, our findings suggest that stability-based laws capture a core structural constraint of mod-  
506 ern overparameterized learning. Developing efficient estimators, stronger empirical validation, and  
507 deeper theoretical connections (e.g., with sharpness and optimization bias) are promising next steps  
508 toward a unified understanding of generalization and robustness.

509

510

511

512

513

514

515

516

517

518

519

520

521

522

523

524

525

526

527

528

529

530

531

532

533

534

535

536

537

538

539

540  
541 ETHICS STATEMENT542  
543 This work focuses on the theoretical analysis of generalization in machine learning and does not  
544 involve experiments on human subjects, sensitive personal data, or applications with direct societal  
545 risks. The datasets referenced are publicly available, and no private or restricted data was used.  
546 Potential ethical concerns related to misuse are minimal, as the contributions are mainly theoretical  
547 and methodological.548 **Acknowledgment of LLM Use.** We explicitly acknowledge that large language models (LLMs)  
549 were used solely for polishing code, improving sentence clarity, and refining grammar. They were  
550 not used for generating research ideas, proofs, or results.552  
553 REPRODUCIBILITY STATEMENT554  
555 We have taken multiple steps to ensure reproducibility of our results. All theoretical claims are  
556 accompanied by rigorous proofs, presented in detail in the appendix. Assumptions underlying the  
557 theorems are explicitly stated, and definitions are given in full to allow independent verification. In  
558 addition, we provide open-source code to reproduce illustrative experiments and examples, which is  
559 available anonymously at anonymous GitHub.560 REFERENCES  
561562 Peter Bartlett, Dylan J. Foster, and Matus Telgarsky. Spectrally-normalized margin bounds for neural  
563 networks, 2017. URL <https://arxiv.org/abs/1706.08498>.564 Peter L Bartlett and Shahar Mendelson. Rademacher and gaussian complexities: Risk bounds and  
565 structural results. *Journal of Machine Learning Research*, 3(Nov):463–482, 2002.566 Peter L Bartlett, Philip M Long, Gábor Lugosi, and Alexander Tsigler. Benign overfitting in linear  
567 regression. *Proceedings of the National Academy of Sciences*, 117(48):30063–30070, 2020.568 Mikhail Belkin, Daniel Hsu, Siyuan Ma, and Soumik Mandal. Reconciling modern machine-  
569 learning practice and the classical bias–variance trade-off. *Proceedings of the National Academy  
570 of Sciences*, 116(32):15849–15854, 2019.571 Simone Bombari, Shayan Kiyani, and Marco Mondelli. Beyond the universal law of robustness:  
572 Sharper laws for random features and neural tangent kernels, 2023. URL <https://arxiv.org/abs/2302.01629>.573 Olivier Bousquet and André Elisseeff. Stability and generalization. *Journal of machine learning  
574 research*, 2(Mar):499–526, 2002.575 Tom Brown, Benjamin Mann, Nick Ryder, Melanie Subbiah, Jared D Kaplan, Prafulla Dhari-  
576 wal, Arvind Neelakantan, Pranav Shyam, Girish Sastry, Amanda Askell, Sandhini Agar-  
577 wal, Ariel Herbert-Voss, Gretchen Krueger, Tom Henighan, Rewon Child, Aditya Ramesh,  
578 Daniel Ziegler, Jeffrey Wu, Clemens Winter, Chris Hesse, Mark Chen, Eric Sigler, Mateusz  
579 Litwin, Scott Gray, Benjamin Chess, Jack Clark, Christopher Berner, Sam McCandlish, Alec  
580 Radford, Ilya Sutskever, and Dario Amodei. Language models are few-shot learners. In  
581 H. Larochelle, M. Ranzato, R. Hadsell, M.F. Balcan, and H. Lin (eds.), *Advances in Neu-  
582 ral Information Processing Systems*, volume 33, pp. 1877–1901. Curran Associates, Inc.,  
583 2020. URL [https://proceedings.neurips.cc/paper\\_files/paper/2020/file/1457c0d6bfcb4967418bfb8ac142f64a-Paper.pdf](https://proceedings.neurips.cc/paper_files/paper/2020/file/1457c0d6bfcb4967418bfb8ac142f64a-Paper.pdf).584 Sébastien Bubeck and Mark Sellke. A universal law of robustness via isoperimetry. *Advances in  
585 Neural Information Processing Systems*, 34:28811–28822, 2021.586 Louis Béthune, Thibaut Boissin, Mathieu Serrurier, Franck Mamalet, Corentin Friedrich, and Al-  
587 berto González-Sanz. Pay attention to your loss: understanding misconceptions about 1-lipschitz  
588 neural networks, 2022. URL <https://arxiv.org/abs/2104.05097>.

594 Santanu Das, Jatin Batra, and Piyush Srivastava. A direct proof of a unified law of robustness for  
 595 bregman divergence losses, 2025. URL <https://arxiv.org/abs/2405.16639>.

596

597 Alhussein Fawzi, Omar Fawzi, and Pascal Frossard. Analysis of classifiers' robustness to adversarial  
 598 perturbations, 2016. URL <https://arxiv.org/abs/1502.02590>.

599

600 Pierre Foret, Ariel Kleiner, Hossein Mobahi, and Behnam Neyshabur. Sharpness-aware minimiza-  
 601 tion for efficiently improving generalization. In *International Conference on Learning Represen-  
 602 tations*, 2021. URL <https://openreview.net/forum?id=6TmlmposlrM>.

603

604 Matteo Gamba, Hossein Azizpour, and Mårten Björkman. On the lipschitz constant of deep net-  
 605 works and double descent, 2025. URL <https://arxiv.org/abs/2301.12309>.

606

607 Ruiqi Gao, Tianle Cai, Haochuan Li, Liwei Wang, Cho-Jui Hsieh, and Jason D. Lee. Convergence of  
 608 adversarial training in overparametrized neural networks, 2019. URL <https://arxiv.org/abs/1906.07916>.

609

610 Nikhil Ghosh and Mikhail Belkin. A universal trade-off between the model size, test loss, and  
 611 training loss of linear predictors, 2023. URL <https://arxiv.org/abs/2207.11621>.

612

613 Justin Gilmer, Luke Metz, Fartash Faghri, Samuel S. Schoenholz, Maithra Raghu, Martin Watten-  
 614 berg, and Ian Goodfellow. Adversarial spheres, 2018. URL <https://arxiv.org/abs/1801.02774>.

615

616 Ian J Goodfellow, Jonathon Shlens, and Christian Szegedy. Explaining and harnessing adversarial  
 617 examples. *International Conference on Learning Representations (ICLR)*, 2015. URL <https://arxiv.org/abs/1412.6572>.

618

619 Henry Gouk, Eibe Frank, Bernhard Pfahringer, and Michael J. Cree. Regularisation of neural  
 620 networks by enforcing lipschitz continuity, 2020. URL <https://arxiv.org/abs/1804.04368>.

621

622 Yifan Hao, Yong Lin, Difan Zou, and Tong Zhang. On the benefits of over-parameterization for  
 623 out-of-distribution generalization, 2024. URL <https://arxiv.org/abs/2403.17592>.

624

625 Jordan Hoffmann, Sébastien Borgeaud, Arthur Mensch, Elena Buchatskaya, Trevor Cai, Eliza  
 626 Rutherford, Diego de Las Casas, Lisa Anne Hendricks, Johannes Welbl, Aidan Clark, Tom Hen-  
 627 nigan, Eric Noland, Katie Millican, George van den Driessche, Bogdan Damoc, Aurelia Guy,  
 628 Simon Osindero, Karen Simonyan, Erich Elsen, Jack W. Rae, Oriol Vinyals, and Laurent Sifre.  
 629 Training compute-optimal large language models, 2022. URL <https://arxiv.org/abs/2203.15556>.

630

631 Yiding Jiang, Behnam Neyshabur, Hossein Mobahi, Dilip Krishnan, and Samy Bengio. Fantastic  
 632 generalization measures and where to find them, 2019. URL <https://arxiv.org/abs/1912.02178>.

633

634 Keller Jordan, Yuchen Jin, Vlado Boza, Jiacheng You, Franz Cesista, Laker Newhouse, and Jeremy  
 635 Bernstein. Muon: An optimizer for hidden layers in neural networks, 2024. URL <https://kellerjordan.github.io/posts/muon/>.

636

637 Guy Katz, Clark Barrett, David Dill, Kyle Julian, and Mykel Kochenderfer. Reluplex: An effi-  
 638 cient smt solver for verifying deep neural networks, 2017. URL <https://arxiv.org/abs/1702.01135>.

639

640 Nitish Shirish Keskar, Dheevatsa Mudigere, Jorge Nocedal, Mikhail Smelyanskiy, and Ping Tak Pe-  
 641 ter Tang. On large-batch training for deep learning: Generalization gap and sharp minima. In  
 642 *International Conference on Learning Representations*, 2017.

643

644 Grigory Khromov and Sidak Pal Singh. Some fundamental aspects about lipschitz continuity of  
 645 neural networks, 2024. URL <https://arxiv.org/abs/2302.10886>.

646

647 Hyunjik Kim, George Papamakarios, and Andriy Mnih. The lipschitz constant of self-attention,  
 648 2021. URL <https://arxiv.org/abs/2006.04710>.

648 Diederik P Kingma and Jimmy Ba. Adam: A method for stochastic optimization. In *3rd International Conference on Learning Representations (ICLR)*, 2015. URL <https://arxiv.org/abs/1412.6980>.

649

650

651 Mojżesz Dawid Kirszbraun. Über die zusammenziehende und lipschitzsche transformationen. *Fundamenta Mathematicae*, 22:77–108, 1934. URL <https://api.semanticscholar.org/CorpusID:117250450>.

652

653

654

655 Jungmin Kwon, Jeongseop Kim, Hyunseo Park, and In Kwon Choi. Asam: Adaptive sharpness-aware minimization for scale-invariant learning of deep neural networks. In Marina Meila and Tong Zhang (eds.), *Proceedings of the 38th International Conference on Machine Learning*, volume 139 of *Proceedings of Machine Learning Research*, pp. 5905–5914. PMLR, 18–24 Jul 2021. URL <https://proceedings.mlr.press/v139/kwon21b.html>.

656

657

658

659

660 Jingwei Li, Jing Xu, Zifan Wang, Huishuai Zhang, and Jingzhao Zhang. Understanding nonlinear implicit bias via region counts in input space, 2025. URL <https://arxiv.org/abs/2505.11370>.

661

662

663

664 Z. N. D. Liu and A. C. Hansen. Do stable neural networks exist for classification problems? – a new view on stability in ai, 2024. URL <https://arxiv.org/abs/2401.07874>.

665

666

667 Aleksander Madry, Aleksandar Makelov, Ludwig Schmidt, Dimitris Tsipras, and Adrian Vladu.

668 Towards deep learning models resistant to adversarial attacks. In *International Conference on Learning Representations (ICLR)*, 2018. URL <https://arxiv.org/abs/1706.06083>.

669

670 Edward James McShane. Extension of range of functions. *Bulletin of the American Mathematical Society*, 40:837–842, 1934. URL <https://api.semanticscholar.org/CorpusID:38462037>.

671

672

673 Seyed-Mohsen Moosavi-Dezfooli, Alhussein Fawzi, and Pascal Frossard. Deepfool: A simple and accurate method to fool deep neural networks. In *IEEE Conference on Computer Vision and Pattern Recognition (CVPR)*, pp. 2574–2582, 2016. doi: 10.1109/CVPR.2016.282.

674

675

676

677 Michael Munn, Benoit Dherin, and Javier Gonzalvo. A margin-based multiclass generalization bound via geometric complexity, 2024. URL <https://arxiv.org/abs/2405.18590>.

678

679

680 Vaishnavh Nagarajan and J. Zico Kolter. Uniform convergence may be unable to explain generalization in deep learning, 2021. URL <https://arxiv.org/abs/1902.04742>.

681

682 Behnam Neyshabur, Zhiyuan Li, Srinadh Bhojanapalli, Yann LeCun, and Nathan Srebro. Towards understanding the role of over-parametrization in generalization of neural networks, 2018. URL <https://arxiv.org/abs/1805.12076>.

683

684

685

686 Adam Paszke, Sam Gross, Francisco Massa, Adam Lerer, James Bradbury, Gregory Chanan, Trevor Killeen, Zeming Lin, Natalia Gimelshein, Luca Antiga, Alban Desmaison, Andreas Kopf, Edward Yang, Zachary DeVito, Martin Raison, Alykhan Tejani, Sasank Chilamkurthy, Benoit Steiner, Lu Fang, Junjie Bai, and Soumith Chintala. Pytorch: An imperative style, high-performance deep learning library. In *Advances in Neural Information Processing Systems 32*, pp. 8024–8035. Curran Associates, Inc., 2019. URL <http://papers.neurips.cc/paper/9015-pytorch-an-imperative-style-high-performance-deep-learning-library.pdf>.

687

688

689

690

691

692

693

694 Jonas Rauber, Wieland Brendel, and Matthias Bethge. Foolbox: A python toolbox to benchmark the robustness of machine learning models. *arXiv preprint arXiv:1707.04131*, 2017. URL <https://arxiv.org/abs/1707.04131>.

695

696

697 Philippe Rigollet and Jan-Christian Hütter. High-dimensional statistics, 2023. URL <https://arxiv.org/abs/2310.19244>.

698

699

700 Shiori Sagawa, Aditi Raghunathan, Pang Wei Koh, and Percy Liang. An investigation of why overparameterization exacerbates spurious correlations. In *Proceedings of the 37th International Conference on Machine Learning*, ICML’20. JMLR.org, 2020.

701

702 Stephan R Sain. The nature of statistical learning theory, 1996.  
 703

704 Amartya Sanyal, Philip H. Torr, and Puneet K. Dokania. Stable rank normalization for improved  
 705 generalization in neural networks and gans. In *International Conference on Learning Representations*, 2020. URL <https://openreview.net/forum?id=H1enKkrFDB>.  
 706

707 Kevin Scaman and Aladin Virmaux. Lipschitz regularity of deep neural networks: analysis and  
 708 efficient estimation, 2019. URL <https://arxiv.org/abs/1805.10965>.  
 709

710 Shai Shalev-Shwartz and Shai Ben-David. *Understanding machine learning: From theory to algo-*  
 711 *rithms*. Cambridge university press, 2014.  
 712

713 Aman Sinha, Hongseok Namkoong, Riccardo Volpi, and John Duchi. Certifying some distribu-  
 714 tional robustness with principled adversarial training, 2020. URL <https://arxiv.org/abs/1710.10571>.  
 715

716 Jure Sokolic, Raja Giryes, Guillermo Sapiro, and Miguel R. D. Rodrigues. Robust large margin  
 717 deep neural networks. *IEEE Transactions on Signal Processing*, 65(16):4265–4280, August 2017.  
 718 ISSN 1941-0476. doi: 10.1109/tsp.2017.2708039. URL <http://dx.doi.org/10.1109/TSP.2017.2708039>.  
 719

720 Jake A. Soloff, Rina Foygel Barber, and Rebecca Willett. Building a stable classifier with the inflated  
 721 argmax, 2025. URL <https://arxiv.org/abs/2405.14064>.  
 722

723 Dimitris Tsipras, Shibani Santurkar, Logan Engstrom, Alexander Turner, and Aleksander Madry.  
 724 Robustness may be at odds with accuracy, 2019. URL <https://arxiv.org/abs/1805.12152>.  
 725

726 Yusuke Tsuzuku, Issei Sato, and Masashi Sugiyama. Lipschitz-margin training: Scalable certifica-  
 727 tion of perturbation invariance for deep neural networks, 2018. URL <https://arxiv.org/abs/1802.04034>.  
 728

729 Roman Vershynin. *High-Dimensional Probability: An Introduction with Applications in Data Sci-  
 730 ence*. Cambridge Series in Statistical and Probabilistic Mathematics. Cambridge University Press,  
 731 2018.

732 Yoav Wald, Gal Yona, Uri Shalit, and Yair Carmon. Malign overfitting: Interpolation can provably  
 733 preclude invariance, 2024. URL <https://arxiv.org/abs/2211.15724>.  
 734

735 Tsui-Wei Weng, Huan Zhang, Hongge Chen, Zhao Song, Cho-Jui Hsieh, Duane Boning, Inderjit S.  
 736 Dhillon, and Luca Daniel. Towards fast computation of certified robustness for relu networks,  
 737 2018. URL <https://arxiv.org/abs/1804.09699>.  
 738

739 Yuezhu Xu and S. Sivanjanji. Eclipse: Efficient compositional lipschitz constant es-  
 740 timation for deep neural networks. In A. Globerson, L. Mackey, D. Belgrave,  
 741 A. Fan, U. Paquet, J. Tomczak, and C. Zhang (eds.), *Advances in Neural In-  
 742 formation Processing Systems*, volume 37, pp. 10414–10441. Curran Associates, Inc.,  
 743 2024. URL [https://proceedings.neurips.cc/paper\\_files/paper/2024/file/1419d8554191a65ea4f2d8e1057973e4-Paper-Conference.pdf](https://proceedings.neurips.cc/paper_files/paper/2024/file/1419d8554191a65ea4f2d8e1057973e4-Paper-Conference.pdf).  
 744

745 Bohang Zhang, Du Jiang, Di He, and Liwei Wang. Rethinking lipschitz neural networks and certified  
 746 robustness: A boolean function perspective, 2022. URL <https://arxiv.org/abs/2210.01787>.  
 747

748 Hongyang Zhang, Yaodong Yu, Jiantao Jiao, Eric P. Xing, Laurent El Ghaoui, and Michael I. Jor-  
 749 dan. Theoretically principled trade-off between robustness and accuracy, 2019. URL <https://arxiv.org/abs/1901.08573>.  
 750

751 Zhenyu Zhu, Fanghui Liu, Grigoris G Chrysos, and Volkan Cevher. Robustness in deep learning:  
 752 The good (width), the bad (depth), and the ugly (initialization), 2023. URL <https://arxiv.org/abs/2209.07263>.  
 753

754 Yingtian Zou, Kenji Kawaguchi, Yingnan Liu, Jiashuo Liu, Mong-Li Lee, and Wynne Hsu. Towards  
 755 robust out-of-distribution generalization bounds via sharpness, 2024. URL <https://arxiv.org/abs/2403.06392>.

756 **A THE NEED FOR ISOPERIMETRY**  
 757

758 Concentration inequalities are essential tools in high-dimensional probability theory, providing  
 759 bounds on the tail behavior of random variables. Next, we outline the key strategy from Bubeck  
 760 & Sellke (Bubeck & Sellke, 2021) for proving the law of robustness for regression, highlighting  
 761 the importance of an additional assumption on the measure  $\mu$ . The authors employ the Lipschitz  
 762 constant of a function as a measure of robustness, where a small Lipschitz constant (i.e.,  $\approx 1$ ) of  
 763 the realization indicates a robust model. The basic idea is to leverage the Lipschitz continuity of  
 764 functions  $f : \mathcal{X} \rightarrow \mathbb{R}$  in conjunction with isoperimetric inequalities to bound the probability

765 
$$\mathbb{P}(\exists f \in \mathcal{F} : \hat{R}_\ell(f) \approx 0 \wedge L(f) \leq L_*) < \delta. \quad (9)$$
  
 766

767 That is, we aim to bound the probability of observing a model that is both robust (i.e., has a small  
 768 Lipschitz constant  $L(f)$ ) and fits the data well (i.e.,  $\hat{R}_\ell(f) \approx 0$ , meaning it nearly interpolates).  
 769 By contraposition, this implies that with probability at least  $1 - \delta$ , the following holds for all  $f \in \mathcal{F}$ :

771 
$$\hat{R}_\ell(f) \approx 0 \implies L(f) > L_*(p, n, d). \quad (10)$$
  
 772

773 Here,  $L_*(p, n, d)$  is an algebraic function of the number of parameters  $p \approx \log |\mathcal{F}|$  (see the paragraph  
 774 below Theorem 4 for details), the number of training samples  $n$ , and the input dimension  $d$ . It  
 775 satisfies  $L_*(p, n, d) \gg 1$  in the non-overparameterized regime  $p \approx n$ , thereby implying non-robust  
 776 behavior.

777 A key ingredient in Bubeck & Sellke (2021) for proving (a variant of) Equation 9 is the isoperimetry  
 778 assumption on the measure  $\mu$ . Isoperimetry, originating in geometry, provides an upper bound  
 779 on a set's volume in terms of its boundary's surface area. In high dimensions, the principle of  
 780 isoperimetry induces a concentration of measure, where the measure of the  $\varepsilon$ -neighborhood  $A_\varepsilon$  of  
 781 any set  $A$  with  $\mu(A) > 0$  has measure  $\mu(A_\varepsilon) \rightarrow 1$ , and the complementary measure decays in the  
 782 order of  $\exp(-d\varepsilon^2)$ . This is equivalent to the sub-Gaussian behavior of every bounded Lipschitz-  
 783 continuous function as stated in Definition 3, yielding a concentration property for  $|f(x) - \mathbb{E}(f)|$   
 784 that depends on the Lipschitz constant  $L(f)$ .

785 The induced concentration property allows us to bound the probability in Equation 9, leveraging the  
 786 intuition that a smaller Lipschitz constant limits the function's capacity to align with random labels.  
 787 However, it is important to note that Equation 10 provides information about robustness within  $\mathcal{F}$   
 788 only if

789 
$$\mathbb{P}(\nexists f \in \mathcal{F} : \hat{R}_\ell(f) \approx 0) \leq 1 - \delta \iff \mathbb{P}(\exists f \in \mathcal{F} : \hat{R}_\ell(f) \approx 0) \geq \delta.$$

790 Otherwise, the implication becomes vacuous, as almost no function in  $\mathcal{F}$  generalizes well, i.e.,  
 791 achieves near-zero empirical risk, to begin with. Without imposing any assumptions on  $\mu$ , Hoeffding's  
 792 inequality already suffices to derive a Lipschitz-independent bound for any function  
 793  $f : \mathcal{X} \rightarrow [-1, 1]$ :

794 
$$\mathbb{P}(|f(x) - \mathbb{E}(f)| \geq t) \leq 2 \exp\left(-\frac{t^2}{2}\right) \quad \forall t > 0. \quad (11)$$
  
 795

796 Thus, to ensure that the probability in Equation 9 remains below  $\delta$  while simultaneously allowing  
 797 for  $\mathbb{P}(\exists f \in \mathcal{F} : \hat{R}_\ell(f) \approx 0) > \delta$ , any concentration inequality relying on the Lipschitz constant  
 798 must exhibit a sufficiently fast decay (in comparison with Equation 11) in the regime  $L(f) \gtrsim 1$ .  
 799 This is necessary to yield a non-vacuous bound in Equation 10, which allows to assess robustness  
 800 by the increase of the minimal Lipschitz constant  $L_*$  even for  $L_* > 1$ .

801 For instance, McDiarmid's inequality applied to Lipschitz functions yields a tail bound of the order  
 802  $\exp\left(-\frac{2t^2}{\text{diam}(\mathcal{X})^2 L(f)^2}\right)$ , which is insufficient as it decays faster than the Hoeffding bound only for  
 803  $L(f) < 2/\text{diam}(\mathcal{X})$ , i.e., at least  $\text{diam}(\mathcal{X}) < 2$  is required to include the (relevant) range  $L(f) > 1$   
 804 of Lipschitz constants. This indicates that a certain restriction of the admissible measures is indeed  
 805 necessary to obtain non-vacuous statements, i.e., they can not be derived in full generality.

806 Notably, the  $c$ -isoperimetry condition in Equation 3 leads to a faster decay than the Hoeffding bound  
 807 in Equation 11 when  $L(f) < \sqrt{dc^{-1}}$ , making it effective for functions with moderate Lipschitz con-  
 808 stants in high-dimensional settings. Our goal is to generalize this strategy to handle discontinuous  
 809 functions, addressing the inherent challenges of classification tasks.

## 810 B THE SIGNED DISTANCE FUNCTION (REMARK 2)

812 We collect the main properties of the signed distance function

$$814 \quad d_f(x) := \begin{cases} 815 \quad d(x, f^{-1}(\{-1\})), & \text{if } f(x) = 1, \\ 816 \quad -d(x, f^{-1}(\{1\})), & \text{if } f(x) = -1, \end{cases}$$

817 where  $d(x, A) := \inf_{y \in A} \|x - y\|_2$ .

818 **Lemma 17.** *Let  $\mathcal{X} \subset \mathbb{R}^d$  be bounded and path-connected, and let  $f : \mathcal{X} \rightarrow \{-1, 1\}$ . Then the*

819 *signed distance function  $d_f$  is 1-Lipschitz.*

820 This is a classical fact, a special case of the Eikonal equation. For completeness, we include a direct

821 proof inspired by Liu & Hansen (2024, Prop. 7.5).

822 *Proof.* **Case 1:**  $f(x) = f(y)$ . Assume w.l.o.g.  $f(x) = f(y) = 1$ . Let  $(z_n)_n$  be a sequence in

823  $f^{-1}(\{-1\})$  with  $|d(y, z_n) - d_f(y)| \leq \frac{1}{n}$ . Then

$$824 \quad \begin{aligned} 825 \quad d_f(x) &= d(x, f^{-1}(\{-1\})) \\ 826 \quad &\leq d(x, z_n) \\ 827 \quad &\leq \|x - y\|_2 + d(y, z_n) \\ 828 \quad &\leq \|x - y\|_2 + d_f(y) + \frac{1}{n}. \end{aligned}$$

829 Letting  $n \rightarrow \infty$  and exploiting symmetry yields  $|d_f(x) - d_f(y)| \leq \|x - y\|_2$ .

830 **Case 2:**  $f(x) \neq f(y)$ . Assume w.l.o.g.  $f(x) = 1, f(y) = -1$ . Consider the line segment  $L =$

831  $\{(1 - t)x + ty : t \in [0, 1]\} \subset \mathcal{X}$  and define

$$832 \quad \begin{aligned} 833 \quad w_1 &= (1 - t_1)x + t_1y, \quad t_1 := \inf\{t : f((1 - t)x + ty) = -1\}, \\ 834 \quad w_2 &= (1 - t_2)x + t_2y, \quad t_2 := \sup\{t : f((1 - t)x + ty) = 1\}. \end{aligned}$$

835 Path-connectedness ensures  $t_1 \leq t_2$ , otherwise the midpoint between  $w_1$  and  $w_2$  would be labeled

836 both 1 and  $-1$ , a contradiction.

837 Thus,

$$838 \quad \begin{aligned} 839 \quad |d_f(x) - d_f(y)| &= d(x, f^{-1}(\{-1\})) + d(y, f^{-1}(\{1\})) \\ 840 \quad &\leq \|x - w_1\|_2 + \|y - w_2\|_2 \\ 841 \quad &\leq \|x - y\|_2. \end{aligned}$$

842  $\square$

843 **Lemma 18.** *Let  $\mathcal{X} \subset \mathbb{R}^d$  and  $f : \mathcal{X} \rightarrow \{-1, 1\}$  with  $f^{-1}(\{1\})$  closed. Then  $f$  can be represented*

844 *as*

$$845 \quad f(x) = \text{sgn}(d_f(x)),$$

846 where we adopt the convention  $\text{sgn}(0) = 1$ .

847 *Proof.* If  $d_f(x) \neq 0$ , the claim follows directly from the definition of  $d_f$ . If  $d_f(x) = 0$ , then

848  $x \in f^{-1}(\{1\})$  by closedness, so  $f(x) = 1 = \text{sgn}(0)$ .  $\square$

849 **Remark 19.** *Lemma 18 justifies the representation  $f = \text{sgn} \circ d_f$  used in the proof of Theorem 4.*

850 *This link between classifiers and their signed distance functions is what allows stability arguments*

851 *to be combined with smoothness-based tools.*

## 852 C PROOF OF THE RADEMACHER BOUND (THEOREM 4)

853 In the regression setting, one can assume without loss of generality that the considered regressors

854 are Lipschitz continuous and thereby derive insightful statements about the expected and feasible

855 robustness of models in a given setting. In contrast, this approach is not meaningful anymore in

856 the classification setting as the considered classifiers are (except for trivial cases) discontinuous

864 by design, i.e., they can not be captured by a finite Lipschitz constant. Thus, statements about the  
 865 robustness of classification models can not be derived via Lipschitz constants. This motivates the use  
 866 of class stability as a replacement measure in the classification setting, which, however, is (inversely)  
 867 related to Lipschitzness as highlighted and exploited in the subsequent proof of Theorem 4. For  
 868 convenience, we repeat the statement with the corresponding assumptions.  
 869

870 (H1)  $(\mathcal{X}, \mu)$  is a probability space with bounded sample space  $\mathcal{X}$  and  $c$ -isoperimetric measure  $\mu$ ;  
 871 (H2) the considered hypothesis class  $\mathcal{F}$  of classifiers  $f : \mathcal{X} \rightarrow \{-1, 1\}$  is finite, that is  $|\mathcal{F}| < \infty$ .

872 **Theorem (Rademacher Bound).** *Suppose Assumptions (H1) and (H2) hold, and that*  
 873  $\min_{f \in \mathcal{F}} S(f) > S > 0$  *with*  $\log |\mathcal{F}| \geq n$ .

875 1. *The empirical Rademacher complexity satisfies*

$$876 \quad 877 \quad 878 \quad \mathcal{R}_{n,\mu}(\mathcal{F}) \leq K_1 \max \left\{ \frac{1}{\sqrt{n}}, \frac{\sqrt{c}}{S} \cdot \frac{\log |\mathcal{F}|}{n\sqrt{d}} \right\}, \quad (12)$$

879 for an absolute constant  $K_1 > 0$ .

880 2. *If, in addition,  $f^{-1}(\{1\})$  is closed and  $\mathcal{X}$  path connected, the bound sharpens to*

$$882 \quad 883 \quad 884 \quad \mathcal{R}_{n,\mu}(\mathcal{F}) \leq K_2 \max \left\{ \frac{1}{\sqrt{n}}, \frac{\sqrt{c}}{S} \sqrt{\frac{\log |\mathcal{F}|}{nd}}, 2 \exp \left( -\frac{dS^2}{8c} \right) \right\}, \quad (13)$$

885 for another absolute constant  $K_2 > 0$ .

886 *Proof.* : 1. To begin, we explore the relationship between two measures of robustness: the Lipschitz  
 887 constant  $L(f)$  and the class stability  $S(f)$  of a  $f \in \mathcal{F}$  on the set  
 888

$$889 \quad A_t(f) := \{x \in \mathcal{X} : h_f(x) > S(f) - t\} \quad \text{for } 0 \leq t \leq S(f).$$

890 Observe that for  $x_1 \in A_t(f)$  and  $x_2 \in \mathcal{X}$

$$892 \quad 893 \quad 894 \quad 895 \quad 896 \quad |f(x_1) - f(x_2)| \leq \begin{cases} 0, & \text{if } f(x_1) = f(x_2) \\ 2 \cdot \underbrace{\frac{\|x_1 - x_2\|}{S(f) - t}}_{\geq 1}, & \text{if } f(x_1) \neq f(x_2) \end{cases} \leq \frac{2}{S(f) - t} \|x_1 - x_2\|,$$

897 i.e.,  $f$  is  $\frac{2}{S(f)-t}$ -Lipschitz on  $A_t(f)$  and, therefore, according to the assumption  $S(f) > S$ , any  
 898  $f \in \mathcal{F}$  is at least  $\frac{2}{S-t}$ -Lipschitz on  $A_t(f)$ . Our strategy now is to apply the Rademacher bound based  
 899 on Lipschitz functions of Bubeck & Sellke in Bubeck & Sellke (2021) to the restriction  $f|_{A_t(f)}$ , and  
 900 additionally exploit isoperimetry to control the measure of the complement  $A_t(f)^c$ . We rely on two  
 901 key facts:

902 • **Fact 1:** Every Lipschitz continuous function  $g : A \rightarrow \mathbb{R}$ , defined on a subset  $A \subset \mathcal{X}$   
 903 of a metric space, can be extended to a function  $G_g : \mathcal{X} \rightarrow \mathbb{R}$ , preserving the same  
 904 Lipschitz constant (McShane (1934), Kirschbraun (1934)).  $\implies$  *This allows us to apply*  
 905 *isoperimetry and thereby the result in (Bubeck & Sellke, 2021, Lemma 4.1) to the  $\frac{2}{S-t}$ -*  
 906 *Lipschitz extension  $F_f$  of  $f|_{A_t(f)}$  (by w.l.o.g. restricting its codomain to  $[-1, 1]$ ) to obtain*

$$908 \quad 909 \quad 910 \quad \frac{1}{n} \mathbb{E}^{\sigma_i, x_i} \left[ \sup_{f \in \mathcal{F}} \left| \sum_{i=1}^n \sigma_i F_f(x_i) \right| \right] \leq C_1 \frac{1}{\sqrt{n}} + C_2 \frac{1}{S-t} \sqrt{\frac{c \log |\mathcal{F}|}{nd}}$$

911 for some absolute constants  $C_1, C_2 > 0$ .

912 • **Fact 2:** The margin  $h_f(x) : \mathcal{X} \rightarrow \mathbb{R}$ , is 1-Lipschitz continuous with respect to the  $\ell_2$ -  
 913 norm (Liu & Hansen, 2024, Prop. 7.5).  $\implies$  *This allows us to control  $\mathbb{P}(A_t(f)^c)$  via*  
 914 *isoperimetry:*

$$916 \quad 917 \quad \mathbb{P}(A_t(f)^c) = \mathbb{P}(\widetilde{S(f)} - h_f(x) \geq t) \leq \exp \left( -\frac{dt^2}{2cL(h_f)^2} \right) = \exp \left( -\frac{dt^2}{2c} \right). \quad (14)$$

918 Via Fact 1, we can bound the Rademacher complexity by  
919

$$\begin{aligned}
920 \quad \mathcal{R}_{n,\mu}(\mathcal{F}) &= \frac{1}{n} \mathbb{E}^{\sigma_i, x_i} \left[ \sup_{f \in \mathcal{F}} \left| \sum_{i=1}^n \sigma_i f(x_i) \right| \right] \\
921 \\
922 \quad &\leq \frac{1}{n} \mathbb{E}^{\sigma_i, x_i} \left[ \sup_{f \in \mathcal{F}} \left| \sum_{i=1}^n \sigma_i F_f(x_i) \right| \right] + \frac{1}{n} \mathbb{E}^{\sigma_i, x_i} \left[ \sup_{f \in \mathcal{F}} \left| \sum_{i=1}^n \sigma_i (f - F_f)(x_i) \right| \right] \\
923 \\
924 \quad &\leq C_1 \frac{1}{\sqrt{n}} + C_2 \frac{1}{S-t} \sqrt{\frac{c \log |\mathcal{F}|}{nd}} + \frac{1}{n} \mathbb{E}^{\sigma_i, x_i} \left[ \sup_{f \in \mathcal{F}} \left| \sum_{i=1}^n \sigma_i (f - F_f)(x_i) \right| \right]. \quad (15)
925 \\
926 \\
927
\end{aligned}$$

928 To control the last term, we subdivide  $\mathcal{X}^n$  into subsets on which specific samples achieve a minimum  
929 margin. To that end, we fix  $t = \frac{S}{2}$  (the exact value is not crucial since it will be subsumed into the  
930 absolute constants) and define, for  $I \subset [n]$ ,

$$931 \quad A^I(f) = A_{\frac{S}{2}}^I(f) := \left\{ x \in \mathcal{X}^n : i \in I \iff h_f(x_i) \geq \frac{S}{2} \right\}.
932 \\
933$$

934 Note, that  $A^{[n]}(f) = A_{\frac{S}{2}}(f)^n$  and  $\cup_{I \in \mathcal{P}([n])} A^I(f)$  is a disjoint partition of  $\mathcal{X}^n$ . Thus, applying a  
935 union bound yields for  $r > 0$

$$\begin{aligned}
936 \quad \mathbb{P} \left( \sup_{f \in \mathcal{F}} \left| \sum_{i=1}^n \sigma_i (f - F_f)(x_i) \right| > r \right) &\leq \sum_{f \in \mathcal{F}} \sum_{I \in \mathcal{P}([n])} \mathbb{P} \left( \left| \sum_{i=1}^n \sigma_i (f - F_f)(x_i) \right| > r \wedge x \in A^I(f) \right) \\
937 \\
938 \quad &= \sum_{f \in \mathcal{F}} \sum_{I \in \mathcal{P}([n])} \mathbb{P} \left( \left| \sum_{i=1}^n \sigma_i (f - F_f)(x_i) \right| > r \mid x \in A^I(f) \right) \mathbb{P}(A^I(f)). \quad (16)
939 \\
940 \\
941
\end{aligned}$$

942 We make the following observations:

- 944 • By construction  $F_f = f$  holds on  $A^I(f)$  for all  $f \in \mathcal{F}$ .
- 945 • As a mean-zero and bounded random variable with range  $[-2, 2]$ ,  $\sigma_i(F_f - f)(x_i)$  is (via  
946 Hoeffding's inequality) subgaussian with variance proxy  $\frac{(2-(-2))^2}{4} = 4$  for every  $i \in [n], f \in \mathcal{F}$ .

947 Using the fact that the sum of  $k$  independent subgaussian random variables with variance proxy  $\sigma^2$   
948 is itself subgaussian with variance proxy  $k\sigma^2$  (Rigollet & Hütter, 2023), we obtain for every  $I \subsetneq [n]$   
949 (the case  $I = [n]$  being trivial) that

$$\begin{aligned}
950 \quad \mathbb{P} \left( \left| \sum_{i=1}^n \sigma_i (f - F_f)(x_i) \right| > r \mid x \in A^I(f) \right) &\leq \mathbb{P} \left( \left| \sum_{i \in I^c} \sigma_i (f - F_f)(x_i) \right| > r \mid x \in A^I(f) \right) \\
951 \\
952 \quad &\leq 2 \exp \left( -\frac{r^2}{2 \cdot 4(n - |I|)} \right).
953 \\
954
\end{aligned}$$

955 On the other hand, we get for  $I \subset [n]$  via Equation 14 that

$$956 \quad \mathbb{P}(A^I(f)) \leq \mathbb{P} \left( \forall j \in I^c : x_j \in A_{\frac{S}{2}}(f)^c \right) = \mathbb{P} \left( x \in A_{\frac{S}{2}}(f)^c \right)^{n-|I|} \leq \exp \left( -\frac{dS^2}{2^3 c} \right)^{n-|I|}.
957 \\
958$$

959 Inserting in Equation 16 and replacing the constants independent of the parameters of interest  
960 ( $n, |\mathcal{F}|, d, r, S$ , and  $|I|$ ) by  $c_1, c_2 > 0$  then gives

$$961 \quad \mathbb{P} \left( \sup_{f \in \mathcal{F}} \left| \sum_{i=1}^n \sigma_i (f - F_f)(x_i) \right| > r \right) \leq \sum_{f \in \mathcal{F}} \sum_{I \in \mathcal{P}([n]) \setminus [n]} 2 \exp \left( -\frac{r^2 c_1}{n - |I|} \right) \exp \left( -\frac{(n - |I|) d S^2 c_2}{c} \right).
962 \\
963 \\
964$$

965 To simplify the above expression, we want to find the maximal term in the sum and use this worst  
966 case as an upper bound over all terms in the sum. To that end, we introduce  $g : [0, n] \rightarrow \mathbb{R}_+$  by

$$967 \quad g(x) = \frac{r^2 c_1}{n - x} + \frac{1}{c} (n - x) S^2 d c_2,
968$$

972 aiming to find its minima, which correspond to an upper bound on the sought worst-case term.  
 973 Differentiating  $g$  yields the extrema  
 974

$$975 \quad g'(x) = \frac{r^2 c_1}{(n-x)^2} - \frac{1}{c} S^2 d c_2 \stackrel{!}{=} 0 \\ 976 \\ 977 \quad \implies x_{+/-} = n \pm \frac{r}{S} \sqrt{\frac{c_1 c}{c_2 d}} =: n \pm \alpha(r) \quad (17) \\ 978 \\ 979$$

980 We calculate the second derivatives to be  $g''(x_-) > 0$  and  $g''(x_+) < 0$ , thus only  $x_-$  is a minimum.  
 981 Now, there are two cases associated with the location of  $x_-$  (taking into account that  $\alpha(r) > 0$  for  
 982 every  $r > 0$ ).  
 983

984

- 985 • **Case I:**  $\alpha(r) \leq n$ .

986 Then,  $x_-$  is a valid minimum in the considered range and therefore  
 987

$$988 \quad \mathbb{P} \left( \sup_{f \in \mathcal{F}} \left| \sum_{i=1}^n \sigma_i(f - F_f)(x_i) \right| > r \right) \\ 989 \\ 990 \quad \leq \sum_{f \in \mathcal{F}} \sum_{I \in \mathcal{P}([n]) \setminus [n]} 2 \exp \left( -\frac{r^2 c_1}{\alpha(r)} \right) \exp \left( -\frac{\alpha(r) d S^2 c_2}{c} \right) \\ 991 \\ 992 \quad \leq 2 |\mathcal{F}| 2^n \exp \left( -2 r S \sqrt{\frac{d c_2 c_1}{c}} \right) := \mathbb{P}_{(I)}(r). \\ 993 \\ 994 \\ 995 \\ 996 \\ 997$$

- 998 • **Case II:**  $\alpha(r) > n$ .

999 Then,  $x_- < 0$  is outside of the domain of  $g$ . However, the derivative satisfies  $g'(x) > 0$  for  
 1000 any  $0 \leq x < n$  since  $x_+ > n$ . Therefore,  $g$  necessarily takes its minimal value at  $x = 0$  so  
 1001 that

$$1002 \quad \mathbb{P} \left( \sup_{f \in \mathcal{F}} \left| \sum_{i=1}^n \sigma_i(f - F_f)(x_i) \right| > r \right) \\ 1003 \\ 1004 \quad \leq \sum_{f \in \mathcal{F}} \sum_{I \in \mathcal{P}([n]) \setminus [n]} 2 \exp \left( -\frac{r^2 c_1}{n} \right) \exp \left( -\frac{n d S^2 c_2}{c} \right) \\ 1005 \\ 1006 \quad \leq 2 |\mathcal{F}| 2^n \exp \left( -\frac{r^2 c_1}{n} \right) \exp \left( -\frac{n d S^2 c_2}{c} \right) =: \mathbb{P}_{(II)}(r). \\ 1007 \\ 1008 \\ 1009 \\ 1010 \\ 1011$$

1012 Using Equation 17, condition  $\alpha(r) > n$  is equivalent to  $r > n S \sqrt{\frac{c_2 d}{c_1 c}}$ . In this range, we have  
 1013  $\mathbb{P}_{(II)}(r) \leq \mathbb{P}_{(I)}(r)$  since  
 1014

$$1015 \quad \mathbb{P}_{(II)} \left( n S \sqrt{\frac{c_2 d}{c_1 c}} \right) = 2 |\mathcal{F}| 2^n \exp \left( -2 n S^2 d c^{-1} c_2 \right) = \mathbb{P}_{(I)} \left( n S \sqrt{\frac{c_2 d}{c_1 c}} \right)$$

1018 and one verifies that  $\mathbb{P}_{(II)}(r)$  decays faster than  $\mathbb{P}_{(I)}(r)$  when further increasing  $r$ . Therefore, we  
 1019 conclude that for all  $r > 0$   
 1020

$$1021 \quad \mathbb{P} \left( \sup_{f \in \mathcal{F}} \left| \sum_{i=1}^n \sigma_i(f - F_f)(x_i) \right| > r \right) \leq \mathbb{P}_{(I)}(r) = 2 |\mathcal{F}| 2^n \exp \left( -2 r S \sqrt{\frac{d c_2 c_1}{c}} \right). \quad (18) \\ 1022 \\ 1023$$

1024 Further rewriting the expression, distinguishing between two cases with respect to the magnitude of  
 1025  $|\mathcal{F}| 2^n$  yields the upper bounds:

1026  
1027 • **Case 1:**  $|\mathcal{F}|2^n \leq \exp\left(rS\sqrt{\frac{dc_2c_1}{c}}\right)$ .

1028 We immediately obtain via Equation 18 that

1029  
1030 
$$\mathbb{P}\left(\sup_{f \in \mathcal{F}} \left| \sum_{i=1}^n \sigma_i(f - F_f)(x_i) \right| > r\right) \leq 2|\mathcal{F}|2^n \exp\left(-2rS\sqrt{\frac{dc_2c_1}{c}}\right)$$
  
1031  
1032  
1033  
1034  
1035  
1036  
1037  
1038  
1039  
1040

$$\leq 2 \exp\left(-rS\sqrt{\frac{dc_2c_1}{c}}\right)$$

$$\leq 2 \exp\left(-\underbrace{\frac{2}{3\log(|\mathcal{F}|2^n)} rS\sqrt{\frac{dc_2c_1}{c}}}_{<1}\right).$$

1041 • **Case 2:**  $|\mathcal{F}|2^n > \exp\left(rS\sqrt{\frac{dc_2c_1}{c}}\right)$ .

1042 In this case, the probability is trivially bounded by

1043  
1044  
1045  
1046  
1047  
1048  
1049

$$\mathbb{P}\left(\sup_{f \in \mathcal{F}} \left| \sum_{i=1}^n \sigma_i(f - F_f)(x_i) \right| > r\right) \leq 1 < 2 \exp\left(-\frac{2}{3}\right) < 2 \exp\left(-\frac{2}{3} \underbrace{\frac{rS\sqrt{\frac{dc_2c_1}{c}}}{\log(|\mathcal{F}|2^n)}}_{<1}\right)$$

1050 Putting both cases together, we proved that for all  $r > 0$

1051  
1052  
1053  
1054

$$\mathbb{P}\left(\sup_{f \in \mathcal{F}} \left| \sum_{i=1}^n \sigma_i(f - F_f)(x_i) \right| > r\right) \leq 2 \exp\left(-\frac{2S\sqrt{\frac{dc_2c_1}{c}}}{3\log(|\mathcal{F}|2^n)} r\right).$$

1055 This tail bound shows that  $\sup_{f \in \mathcal{F}} |\sum_{i=1}^n \sigma_i(f - F_f)(x_i)|$  is sub-exponential. Since the expected  
1056 value of any sub-exponential random variable is up to an absolute constant given by its sub-  
1057 exponential norm, which corresponds (up to a constant) to the parameter  $\frac{3\log(|\mathcal{F}|2^n)}{2S\sqrt{\frac{dc_2c_1}{c}}}$  in the tail  
1058 bound Vershynin (2018), we obtain for a constant  $C_3 > 0$  that

1059  
1060  
1061  
1062  
1063

$$\frac{1}{n} \mathbb{E}^{\sigma_i, x_i} \left[ \sup_{f \in \mathcal{F}} \left| \sum_{i=1}^n \sigma_i(f - F_f)(x_i) \right| \right] \leq C_3 \frac{1}{S} \left( \frac{\log |\mathcal{F}| + n \log 2}{n \sqrt{\frac{d}{c}}} \right)$$

1064 Finally, the desired bound on the Rademacher complexity follows via Equation 15:

1065  
1066  
1067  
1068  
1069  
1070  
1071

$$\begin{aligned} \mathcal{R}_{n,\mu}(\mathcal{F}) &= \frac{1}{n} \mathbb{E}^{\sigma_i, x_i} \left[ \sup_{f \in \mathcal{F}} \left| \sum_{i=1}^n \sigma_i f(x_i) \right| \right] \\ &\leq C_1 \frac{1}{\sqrt{n}} + C_2 \frac{1}{S} \sqrt{\frac{c \log |\mathcal{F}|}{nd}} + C_3 \frac{1}{S} \frac{\sqrt{c} \log |\mathcal{F}|}{n \sqrt{d}} + C_3 \frac{1}{S} \sqrt{\frac{c}{d}}, \end{aligned}$$

1072 which, with the additional assumption  $\log |\mathcal{F}| \geq n$ , gives the result in 1.

1073 **2.** By Lemma 18, every  $f$  admits the representation  $f = \text{sgn} \circ d_f$ . This lets us follow the infinite-  
1074 class analysis (presented in detail in the proof of Theorem 13), without the  $\varepsilon$ -net step in Equation 22.  
1075 From Lemma 17,  $d_f$  is 1-Lipschitz, i.e.,  $L(d_f) = 1$  under the given conditions. Furthermore,  
1076 recalling the co-stability definition we get

1077  
1078  
1079

$$S^*(d_f) = \mathbb{E}[|d_f|] = \mathbb{E}[h_f] = S(f).$$

Plugging this into the general bound in Equation 8 gives the result.  $\square$

1080 C.1 COMPARISON TO STANDARD BOUND WITHOUT ACCOUNTING FOR STABILITY  
1081

1082 Note that the crucial expectation in the derivation, i.e., the last term in Equation 15, can be treated  
1083 without linking it to the minimum class stability. Indeed, the expectation of the maximum of  $N$   
1084 subgaussians  $X_1, \dots, X_N$  with variance proxy  $\sigma^2$  scales as

$$1085 \mathbb{E} \left[ \max_{1 \leq i \leq N} |X_i| \right] \leq \sigma \sqrt{2 \log(2N)}, \quad (19)$$

1088 see for instance Rigollet & Hütter (2023). Hence, in our case, as  $\sigma_i(f - F_f)(x_i)$  is subgaussian  
1089 with variance proxy 4 and therefore  $\sum_{i=1}^n \sigma_i(f - F_f)(x_i)$  is subgaussian with variance proxy  $4n$ ,  
1090 we obtain

$$1091 \frac{1}{n} \mathbb{E}^{\sigma_i, x_i} \left[ \sup_{f \in \mathcal{F}} \left| \sum_{i=1}^n \sigma_i(f - F_f)(x_i) \right| \right] \leq \frac{1}{n} 2\sqrt{n} \sqrt{2 \log(2|\mathcal{F}|)} \leq C_4 \left( \sqrt{\frac{1}{n}} + \sqrt{\frac{\log |\mathcal{F}|}{n}} \right).$$

1094 for some absolute constant  $C_4 > 0$ . Neglecting the constants, this leads to the following comparison  
1095 to our bound in Equation 5:

$$1096 \frac{\sqrt{c}}{S} \sqrt{\frac{p}{nd}} \leq \sqrt{\frac{\log |\mathcal{F}|}{n}} \iff S \geq \sqrt{\frac{c}{d}}.$$

1099 Thus, under the isoperimetry condition, our bound improves on the standard Rademacher complex-  
1100 ity estimate whenever the class stability  $S$  exceeds  $\sqrt{c/d}$ , a mild requirement in high-dimensional  
1101 settings.

## 1103 D PROOF OF THE LAW OF ROBUSTNESS (COROLLARY 6)

1105 Next, we provide the proof of Corollary 6, which we repeat for convenience.

1107 **Theorem** (Law of Robustness for Discontinuous Functions). *Assume (H1), (H2), and the additional  
1108 conditions in 2. of Theorem 4 hold. Let  $p := \log |\mathcal{F}| \geq n$ . Fix  $\varepsilon, \delta \in (0, 1)$  and consider the 0–1  
1109 loss  $\ell_{0-1}$ . There exists an absolute constant  $K > 0$  such that, if*

1110 1. the minimal risk  $\sigma^2 := \min_{f \in \mathcal{F}} R_{0-1}(f)$  satisfies  $\sigma^2 \geq \varepsilon$ , and

1112 2. the sample size  $n$  is large enough to ensure (i)  $\frac{K}{\sqrt{n}} < \frac{\varepsilon}{3}$  and (ii)  $\sqrt{\frac{2 \log(2/\delta)}{n}} < \frac{\varepsilon}{2}$ ,

1114 then with probability at least  $1 - \delta$  (over the sample), the following holds uniformly for all  $f \in \mathcal{F}$ :

$$1116 \hat{R}_{0-1}(f) \leq \sigma^2 - \varepsilon \implies S(f) < \max \left\{ \frac{3K}{\varepsilon} \sqrt{\frac{c \log |\mathcal{F}|}{nd}}, \sqrt{\frac{8c}{d} \log \left( \frac{6K}{\varepsilon} \right)} \right\}.$$

1119 *Proof.* Let  $K > 0$  be an absolute constant such that Equation 5 holds, and define the threshold  
1120 stability

$$1122 S_* = S_*(p, n, d, \varepsilon) := \max \left\{ \frac{3K}{\varepsilon} \sqrt{\frac{c \log |\mathcal{F}|}{nd}}, \sqrt{\frac{8c}{d} \log \left( \frac{6K}{\varepsilon} \right)} \right\}.$$

1124 Then, Theorem 4, together with condition 2(i), implies that

$$1126 \mathcal{R}_{n,\mu}(\mathcal{F}_{S_*}) \leq K \max \left\{ \frac{1}{\sqrt{n}}, \frac{\sqrt{c}}{S_*} \sqrt{\frac{\log |\mathcal{F}|}{nd}}, 2 \exp \left( - \frac{dS_*^2}{8c} \right) \right\} \leq \varepsilon/3,$$

1129 where  $\mathcal{F}_{S_*} := \{f \in \mathcal{F} : S(f) \geq S_*\}$  is the subset of functions in  $\mathcal{F}$  with stability at least  $S_*$ .  
1130 Hence, applying the generalization inequality Equation 1, together with condition 2(ii), gives with  
1131 probability  $1 - \delta$ :

$$1133 \sup_{f \in \mathcal{F}_{S_*}} (R_{0-1}(f) - \hat{R}_{0-1}(f)) \leq 2\mathcal{R}_{n,\mu}(\ell_{0-1} \circ \mathcal{F}_{S_*}) + \sqrt{\frac{2 \log(2/\delta)}{n}} \leq \mathcal{R}_{n,\mu}(\mathcal{F}_{S_*}) + \frac{\varepsilon}{2} < \varepsilon,$$

1134 where we additionally used Equation 2 in the second step. In particular, we can bound the probability  
 1135

$$1136 \mathbb{P}(\forall f \in \mathcal{F}_{S_*} : \hat{R}_{0-1}(f) > \sigma^2 - \varepsilon) \geq \mathbb{P}(\forall f \in \mathcal{F}_{S_*} : R_{0-1}(f) - \hat{R}_{0-1}(f) < \varepsilon) \geq 1 - \delta,$$

1137 where the first inequality follows from  
 1138

$$1139 R_{0-1}(f) - \hat{R}_{0-1}(f) < \varepsilon \stackrel{\text{condition 1.}}{\implies} \sigma^2 - \hat{R}_{0-1}(f) < \varepsilon \implies \hat{R}_{0-1}(f) > \sigma^2 - \varepsilon.$$

1140 Decomposing this probability into two disjoint events  
 1141

$$1142 1 - \delta \leq \mathbb{P}(\forall f \in \mathcal{F}_{S_*} : \hat{R}_{0-1}(f) > \sigma^2 - \varepsilon) = \mathbb{P}(\forall f \in \mathcal{F} : \hat{R}_{0-1}(f) > \sigma^2 - \varepsilon) \\ 1143 + \mathbb{P}(\exists f \in \mathcal{F}_{S_*}^c : \hat{R}_{0-1}(f) \leq \sigma^2 - \varepsilon), \quad (20)$$

1144 enables us to easily recognize that the expression exactly characterizes the probability that the following implication, and thereby the result, holds uniformly for all  $f \in \mathcal{F}$ :  
 1145

$$1146 \hat{R}_{0-1}(f) \leq \sigma^2 - \varepsilon \implies S(f) < S_*$$

1147 Indeed, the implication above holds if, for a given data sample  $(x_i, y_i)_{i=1}^n$ , either  
 1148

- 1149 • no function  $f \in \mathcal{F}$  satisfies  $\hat{R}_{0-1}(f) \leq \sigma^2 - \varepsilon$ , or  
 1150
- 1151 • any such  $f$  lies in  $\mathcal{F}_{S_*}^c$ , that is,  $S(f) < S_*$ ,

1152 which is the case with probability at least  $1 - \delta$  due to Equation 20.  $\square$   
 1153

## 1154 E PROOF OF RADEMACHER BOUND FOR INFINITE FUNCTION CLASSES 1155 (THEOREM 13)

1156 Here we show how to extend the result for finite function classes to infinite function classes by a  
 1157 covering argument, where the Lipschitz continuity of the parameterization turns out to be crucial.  
 1158 Please find the exact statement about the Rademacher complexity of infinite function classes (of a  
 1159 certain form) below, after restating our new regularity hypothesis replacing (H2).  
 1160

1161 (H3) The hypothesis class  $\mathcal{F}$  is of the form  $\mathcal{F} = \text{sgn} \circ \mathcal{G}$ , where  $\mathcal{G} = \{g_w : \mathcal{X} \rightarrow [-1, 1] : w \in \mathcal{W}\}$  is a parameterized class of Lipschitz continuous functions. The parameter space  $\mathcal{W} \subset \mathbb{R}^p$  is bounded with  $\text{diam}(\mathcal{W}) \leq \bar{W}$ , and the parameterization is Lipschitz continuous, i.e.,  
 1162

$$1163 \|g_{w_1} - g_{w_2}\|_\infty \leq J \|w_1 - w_2\|.$$

1164 **Theorem.** Under assumptions (H1) and (H3), suppose that  $S^*(g) > S^* > 0$  and  $L(g) \leq L$  for all  
 1165  $g \in \mathcal{G}$ . Furthermore, assume that  $p \geq n$ . Then, for any covering precision  $\tilde{\varepsilon} > 0$ ,  
 1166

$$1167 \mathcal{R}_{n,\mu}(\mathcal{F}) \leq K \max \left\{ \sqrt{\frac{1}{n}}, \frac{L}{S^*} \sqrt{\frac{p}{nd}} \sqrt{c \log(1 + 60WJ\tilde{\varepsilon}^{-1})}, 2 \exp\left(-\frac{dS^{*2}}{8cL^2}\right), \frac{J}{S^*} \tilde{\varepsilon} \right\},$$

1168 where  $K > 0$  is an absolute constant independent of  $p, n, d, S^*, c, L, J, \tilde{\varepsilon}, W$ .  
 1169

1170 *Proof.* Given any discontinuous classifier  $f_w = \text{sgn} \circ g_w$  for  $g_w \in \mathcal{G}$ , define its Lipschitz continuous  
 1171 approximation for  $\gamma > 0$  as  
 1172

$$F_{f_w} = \text{sgn}_\gamma \circ g_w,$$

1173 where  
 1174

$$1175 \text{sgn}_\gamma(t) := \begin{cases} -1, & t \leq -\gamma, \\ \frac{t}{\gamma}, & t \in [-\gamma, \gamma], \\ 1, & t \geq \gamma. \end{cases}$$

1176 This approximation satisfies the useful property that both  $F_{f_w}$  and the absolute difference  $|f_w - F_{f_w}|$   
 1177 are Lipschitz continuous in both the input space  $\mathcal{X}$  and the weight space  $\mathcal{W}$ , with  
 1178

$$1179 L(|\text{sgn}_\gamma \circ g_w - \text{sgn} \circ g_w|) = L(\text{sgn}_\gamma \circ g_w) = \frac{L(g_w)}{\gamma}. \quad (21)$$

Following the same strategy as in the proof of Theorem 4 with Lipschitz continuous approximations introduced above (see Equation 15), coupled with a covering argument as in Bubeck & Sellke (2021), we obtain

$$\begin{aligned}
\mathcal{R}_{n,\mu}(\mathcal{F}) &= \frac{1}{n} \mathbb{E}^{\sigma_i, x_i} \left[ \sup_{f \in \mathcal{F}} \left| \sum_{i=1}^n \sigma_i f(x_i) \right| \right] \\
&\leq \frac{1}{n} \mathbb{E}^{\sigma_i, x_i} \left[ \sup_{f \in \mathcal{F}} \left| \sum_{i=1}^n \sigma_i F_f(x_i) \right| \right] + \frac{1}{n} \mathbb{E}^{\sigma_i, x_i} \left[ \sup_{f \in \mathcal{F}} \left| \sum_{i=1}^n \sigma_i (f - F_f)(x_i) \right| \right] \\
&\leq C_1 \frac{1}{\sqrt{n}} + C_2 \frac{L}{\gamma} \sqrt{\frac{c}{nd} \underbrace{\sqrt{p \log(1 + 60WJ\tilde{\varepsilon}^{-1})}}_{\geq \sqrt{\log |\mathcal{F}|}}} + \frac{1}{n} \mathbb{E}^{\sigma_i, x_i} \left[ \sup_{f \in \mathcal{F}} \left| \sum_{i=1}^n \sigma_i (f - F_f)(x_i) \right| \right].
\end{aligned}$$

Here the parameter  $\tilde{\varepsilon} > 0$  is related to a  $\tilde{\varepsilon}$ -net of  $\mathcal{W}$ , which we denote by  $\mathcal{W}_{\tilde{\varepsilon}}$ . Note, that  $|\mathcal{W}_{\tilde{\varepsilon}}| \leq (1 + 60WJ\tilde{\varepsilon}^{-1})^p$  (see e.g. Vershynin (2018) Corollary 4.2.13) so the same holds true for the induced net  $\mathcal{F}_{\tilde{\varepsilon}} = \{\text{sgn} \circ g_w : w \in \mathcal{W}_{\tilde{\varepsilon}}\}$ , which also allows us to treat the remaining expectation by subdividing the supremum:

$$\begin{aligned}
\frac{1}{n} \mathbb{E}^{\sigma_i, x_i} \left[ \sup_{f \in \mathcal{F}} \left| \sum_{i=1}^n \sigma_i (f - F_f)(x_i) \right| \right] &= \frac{1}{n} \mathbb{E}^{\sigma_i, x_i} \left[ \sup_{w_{\tilde{\varepsilon}} \in \mathcal{W}_{\tilde{\varepsilon}}} \sup_{w \in B_{\tilde{\varepsilon}}(w_{\tilde{\varepsilon}})} \left| \sum_{i=1}^n \sigma_i (f_w - F_{f_w})(x_i) \right| \right] \\
&\leq \frac{1}{n} \mathbb{E}^{x_i} \left[ \sup_{w_{\tilde{\varepsilon}} \in \mathcal{W}_{\tilde{\varepsilon}}} \sum_{i=1}^n |f_{w_{\tilde{\varepsilon}}} - F_{f_{w_{\tilde{\varepsilon}}}}|(x_i) \right] \\
&\quad + \frac{1}{n} \mathbb{E}^{x_i} \left[ \sup_{w_{\tilde{\varepsilon}} \in \mathcal{W}_{\tilde{\varepsilon}}} \sup_{w \in B_{\tilde{\varepsilon}}(w_{\tilde{\varepsilon}})} \sum_{i=1}^n \left| |f_w - F_{f_w}|(x_i) - |f_{w_{\tilde{\varepsilon}}} - F_{f_{w_{\tilde{\varepsilon}}}}|(x_i) \right| \right]. \tag{22}
\end{aligned}$$

By Lipschitz continuity of the parameterization and of  $|f - F_f|$  as derived in Equation 21, we obtain

$$\| |f_w - F_{f_w}| - |f_{w_{\tilde{\varepsilon}}} - F_{f_{w_{\tilde{\varepsilon}}}}| \|_{\infty} \leq \frac{J}{\gamma} \tilde{\varepsilon} \quad \text{for any } w_{\tilde{\varepsilon}} \in \mathcal{W}_{\tilde{\varepsilon}} \text{ and } w \in B_{\tilde{\varepsilon}}(w_{\tilde{\varepsilon}})$$

so that

$$\frac{1}{n} \mathbb{E}^{x_i} \left[ \sup_{w_{\tilde{\varepsilon}} \in \mathcal{W}_{\tilde{\varepsilon}}} \sup_{w \in B_{\tilde{\varepsilon}}(w_{\tilde{\varepsilon}})} \sum_{i=1}^n \left| |f_w - F_{f_w}|(x_i) - |f_{w_{\tilde{\varepsilon}}} - F_{f_{w_{\tilde{\varepsilon}}}}|(x_i) \right| \right] \leq \frac{J}{\gamma} \tilde{\varepsilon}.$$

Via isoperimetry and using the same bound on the cardinality of  $\mathcal{F}_{\tilde{\varepsilon}}$  as before, one concludes that the first expectation in Equation 22 is of the same form as Equation 19 with subgaussian variance proxy  $\sigma^2 = \frac{L^2}{\gamma^2} \frac{cn}{d}$  so that

$$\begin{aligned}
\frac{1}{n} \mathbb{E}^{x_i} \left[ \sup_{w_{\tilde{\varepsilon}} \in \mathcal{W}_{\tilde{\varepsilon}}} \sum_{i=1}^n |f_{w_{\tilde{\varepsilon}}} - F_{f_{w_{\tilde{\varepsilon}}}}|(x_i) \right] &= \frac{1}{n} \mathbb{E}^{x_i} \left[ \sup_{w_{\tilde{\varepsilon}} \in \mathcal{W}_{\tilde{\varepsilon}}} \sum_{i=1}^n |f_{w_{\tilde{\varepsilon}}} - F_{f_{w_{\tilde{\varepsilon}}}}|(x_i) - \mathbb{E}[|f_{w_{\tilde{\varepsilon}}} - F_{f_{w_{\tilde{\varepsilon}}}}|] \right] \\
&\quad + \sup_{w_{\tilde{\varepsilon}} \in \mathcal{W}_{\tilde{\varepsilon}}} \mathbb{E}[|f_{w_{\tilde{\varepsilon}}} - F_{f_{w_{\tilde{\varepsilon}}}}|] \\
&\leq C_3 \frac{L}{\gamma} \sqrt{\frac{c}{nd} \sqrt{p \log(1 + 60WJ\tilde{\varepsilon}^{-1})}} + \sup_{w_{\tilde{\varepsilon}} \in \mathcal{W}_{\tilde{\varepsilon}}} \mathbb{E}[|f_{w_{\tilde{\varepsilon}}} - F_{f_{w_{\tilde{\varepsilon}}}}|].
\end{aligned}$$

Finally, for every  $f \in \mathcal{F}$ ,

$$\mathbb{E}[|f - F_f|] = \int_{\mathcal{X}} |f(x) - F_f(x)| d\mu(x) \leq \mathbb{P}(g(x) \in [-\gamma, \gamma]). \tag{23}$$

1242 Choosing  $\gamma = \frac{S^*(g)}{2}$ , we obtain by the definitions of co-margin, and once again isoperimetry (since  
1243 the co-margin inherits the Lipschitzness from  $g$  by design)

$$\begin{aligned} 1245 \quad \mathbb{P}(g(x) \in [-\gamma, \gamma]) &= \mathbb{P}\left(|g(x)| \leq \frac{S^*(g)}{2}\right) \\ 1246 \quad &\leq \mathbb{P}\left(|h_g^*(x) - S^*(g)| \geq \frac{S^*(g)}{2}\right) \\ 1247 \quad &\leq 2 \exp\left(-\frac{d S^*(g)^2}{8cL(g)^2}\right) \leq 2 \exp\left(-\frac{d S^{*2}}{8cL^2}\right) = 2 \exp\left(-\frac{d \bar{S}^{*2}}{8c}\right). \\ 1248 \quad & \\ 1249 \quad & \\ 1250 \quad & \\ 1251 \quad & \end{aligned}$$

1252 Putting it all together, we have

$$1253 \quad \mathcal{R}_{n,\mu}(\mathcal{F}) \leq C_1 \frac{1}{\sqrt{n}} + C'_2 \frac{L}{S^*} \sqrt{\frac{c}{nd}} \sqrt{p \log(1 + 60WJ\tilde{\varepsilon}^{-1})} + \frac{2J}{S^*} \tilde{\varepsilon} + 2 \exp\left(-\frac{d S^{*2}}{8cL^2}\right).$$

□

## 1258 F MULTI-CLASS CLASSIFICATION

1260 In this section, we briefly outline how our results extend to categorical distributions with  $\mathcal{C} \in \mathbb{N}$   
1261 classes. We assume that a classifier is given by

$$1263 \quad f : \mathcal{X} \rightarrow \{0, 1\}^{\mathcal{C}},$$

1264 with exactly one non-zero entry for each  $x \in \mathcal{X}$ . The additional regularity assumption (H3)', the  
1265 adaptations of the conditions in (H3) to the multi-class setting can be formalized as follows.

1266 (H3)' The hypothesis class has the form  $\mathcal{F} = \text{argmax } \mathcal{G}$ , where  $\mathcal{G} = \{g_w : \mathcal{X} \rightarrow [0, 1]^{\mathcal{C}} : w \in \mathcal{W}\}$  is a parameterized family of Lipschitz functions. The parameter space  $\mathcal{W} \subset \mathbb{R}^p$  is  
1267 bounded with  $\text{diam}(\mathcal{W}) \leq \bar{W}$ , and the parameterization is Lipschitz:

$$1268 \quad \|g_{w_1} - g_{w_2}\|_{\infty} \leq J \|w_1 - w_2\|.$$

1269 Thus, we can interpret  $g \in \mathcal{G}$  as representing the class probabilities.

1270 **Remark 20.** For binary classification, i.e.  $\mathcal{C} = 2$ , the classifiers are of the form  $f : \mathcal{X} \rightarrow \{0, 1\}^2$ ,  
1271 instead of  $f : \mathcal{X} \rightarrow \{-1, 1\}$ , as considered earlier. However, one can translate between these  
1272 representations by post-composing with either

$$1273 \quad \alpha(x_1, x_2) := x_1 - x_2 \quad \text{or} \quad \beta(x) := \left(\frac{x+1}{2}, \frac{1-x}{2}\right).$$

1274 By the contraction principle for Rademacher complexity, it is therefore sufficient to compute the  
1275 complexity for one of these models.

1276 As in the binary case, our proofs start by considering the Rademacher complexity of the function  
1277 class  $\mathcal{F}$ :

$$1278 \quad \mathcal{R}_{n,\mu}(\mathcal{F}) = \frac{1}{n} \mathbb{E}^{\sigma_{ij}, x_i} \left[ \sup_{f \in \mathcal{F}} \left| \sum_{i=1}^n \sum_{j=1}^{\mathcal{C}} \sigma_{ij} f_j(x_i) \right| \right] \leq \sum_{j=1}^{\mathcal{C}} \frac{1}{n} \mathbb{E}^{\sigma_{ij}, x_i} \left[ \sup_{f \in \mathcal{F}} \left| \sum_{i=1}^n \sigma_{ij} f_j(x_i) \right| \right].$$

1279 Each summand corresponds to a binary classification problem with a one-vs-all classifier  $f_j$ . Indeed,  
1280  $f_j$  is  $\frac{2}{S(f)-t}$ -Lipschitz on  $A_t(f)$ . Transforming via

$$1281 \quad f_j \mapsto 2f_j - 1 : \mathcal{X} \rightarrow \{-1, 1\},$$

1282 we can follow the same reasoning as in Appendix C, obtaining, up to a linear factor of  $\mathcal{C}$ , the same  
1283 result as the first part of Theorem 4, generalized to the multi-class setting.

1284 Similarly, under assumption (H3), we can write

$$1285 \quad 2f_j - 1 = \text{sgn}(g_j - \max_{i \neq j} g_i(x)),$$

1296

Table 1: Multi-class definitions.

1297

1298

1299

1300

1301

1302

1303

1304

1305

1306

1307

1308

1309

1310

1311

1312

1313

1314

1315

Concept	Definition
Isoperimetry	$\mathbb{P}(\ f(x) - \mathbb{E}[f]\ _\infty \geq t) \leq 2 \exp\left(-\frac{dt^2}{2cL^2}\right)$
Rademacher complexity	$\mathcal{R}_{n,\mu}(\mathcal{F}) = \frac{1}{n} \mathbb{E}^{\sigma_{i,j}, x_i} \left[ \sup_{f \in \mathcal{F}} \left  \sum_{i=1}^n \sum_{j=1}^C \sigma_{ij} f_j(x_i) \right  \right]$
Margin	$h_f(x) = \sum_{j=1}^C h_f^j(x), \quad h_f^j(x) := \inf\{\ x - z\ _2 : f(z) \neq j, z \in \mathbb{R}^d\}$
Class stability	$S(f) = \sum_{j=1}^C S(f)^j, \quad S(f)^j := \mathbb{E}[h_f^j]$
Co-margin	$h_g^*(x) = \sum_{j=1}^C h_g^{*j}(x), \quad h_g^{*j}(x) := \max(0, g_j(x) - \max_{i \neq j} g_i(x))$
Co-stability	$S^*(g) = \sum_{j=1}^C S^{*j}(g), \quad S^{*j}(g) := \mathbb{E}[h_g^{*j}]$

which allows us to proceed as in Appendix E to obtain a multi-class generalization of the second part of Theorem 4 and Theorem 13. The only minor difference lies in bounding the term in Equation 23:

$$\mathbb{E}[|f_j - F_{f_j}|] \leq \mathbb{P}[|g_j(x) - \max_{i \neq j} g_i(x)| \leq \gamma].$$

Choosing  $\gamma = \frac{S^*(g)}{2}$ , we use that for all  $j$ ,  $|g_j(x) - \max_{i \neq j} g_i(x)| > h_g^*(x)$ , which yields

$$\begin{aligned} \mathbb{P}[|g_j(x) - \max_{i \neq j} g_i(x)| \leq \frac{S^*(g)}{2}] &\leq \mathbb{P}[|h_g^*(x) - S^*(f)| \geq \frac{S^*(g)}{2}] \\ &\leq 2 \exp\left(-\frac{d S^*(g)^2}{8cL(g)^2}\right) \\ &\leq 2 \exp\left(-\frac{d S^{*2}}{8cL^2}\right) = 2 \exp\left(-\frac{d \bar{S}^{*2}}{8c}\right). \end{aligned}$$

We conclude that all of our results extend to the multi-class case. Moreover, the measure used in our MNIST and CIFAR-10 experiments (Section 6) is the correct generalization.

## G EXPERIMENTAL DETAILS FOR STABILITY MEASUREMENT

**Training setup.** To empirically validate our robustness law, we trained fully connected MLPs on MNIST and CIFAR-10 datasets. Each model has 4 hidden layers with widths  $w \in \{128, 256, 512, 1024, 2048\}$  for MNIST and up to  $w = 1024$  for CIFAR10. All models use ReLU activations, batch normalization, and were initialized with standard parametrization. Training was conducted using the Adam optimizer (Kingma & Ba, 2015) for the embedding and output layers, and the Muon optimizer (Jordan et al., 2024) for the hidden layers. Models were trained with a batch size of 256 and learning rate  $10^{-3}$ , until at least 99% training accuracy was achieved, ensuring (near) interpolation. We further used sharpness-aware optimization based on (Foret et al., 2021; Kwon et al., 2021) to reduce variance of the normalized co-stability on MNIST.

**Parameter counts and normalization.** For each model, we recorded the total number of trainable parameters  $p$ , input dimension  $d$ , and total number of training samples  $n$ .

**Stability estimation.** Class stability  $S(f)$  was computed using adversarial perturbation analysis. We performed a suite of  $\ell_2$ -based attacks (FGSM, PGD, DeepFool, and L2PGD (Goodfellow et al., 2015; Moosavi-Dezfooli et al., 2016; Madry et al., 2018)) using the Foolbox library (Rauber et al., 2017). For each input  $x$ , we recorded the minimum perturbation norm required to change the classifier’s prediction, over a grid of radii  $\mathbf{r} = (0.002, 0.01, 0.05, 0.1, 1, 2)$ . The final stability score  $S(f)$  was taken as the average  $\ell_2$  distance across the dataset.

1350  
 1351     **Normalized Co-Stability estimation.** The empirical co-stability  $S^*(g)$  is computed via the multi-  
 1352     class margin  
 1353         
$$g_j(x) - \max_{i \neq j} g_i(x), \quad j = \arg \max_i g_i(x),$$
  
 1354     averaged over the dataset. We estimate the Lipschitz constant  $L(g)$  using the efficient ECLIPSE  
 1355     method (Xu & Sivarajani, 2024), and report the normalized ratio  $S^*(g)/L(g)$  as a function of  
 1356     model size.  
 1357  
 1358     **Implementation.** Training and evaluation code is implemented in PyTorch (Paszke et al., 2019).  
 1359     For MLPs, images were flattened to vectors. Attack evaluations were conducted over the full dataset  
 1360     (train and test).  
 1361  
 1362     **Reproducibility.** All experiments were run with multiple random seeds  $\{0, 1, 2, 3, 4\}$ , and mean  
 1363     with standard deviation are reported.  
 1364  
 1365  
 1366  
 1367  
 1368  
 1369  
 1370  
 1371  
 1372  
 1373  
 1374  
 1375  
 1376  
 1377  
 1378  
 1379  
 1380  
 1381  
 1382  
 1383  
 1384  
 1385  
 1386  
 1387  
 1388  
 1389  
 1390  
 1391  
 1392  
 1393  
 1394  
 1395  
 1396  
 1397  
 1398  
 1399  
 1400  
 1401  
 1402  
 1403

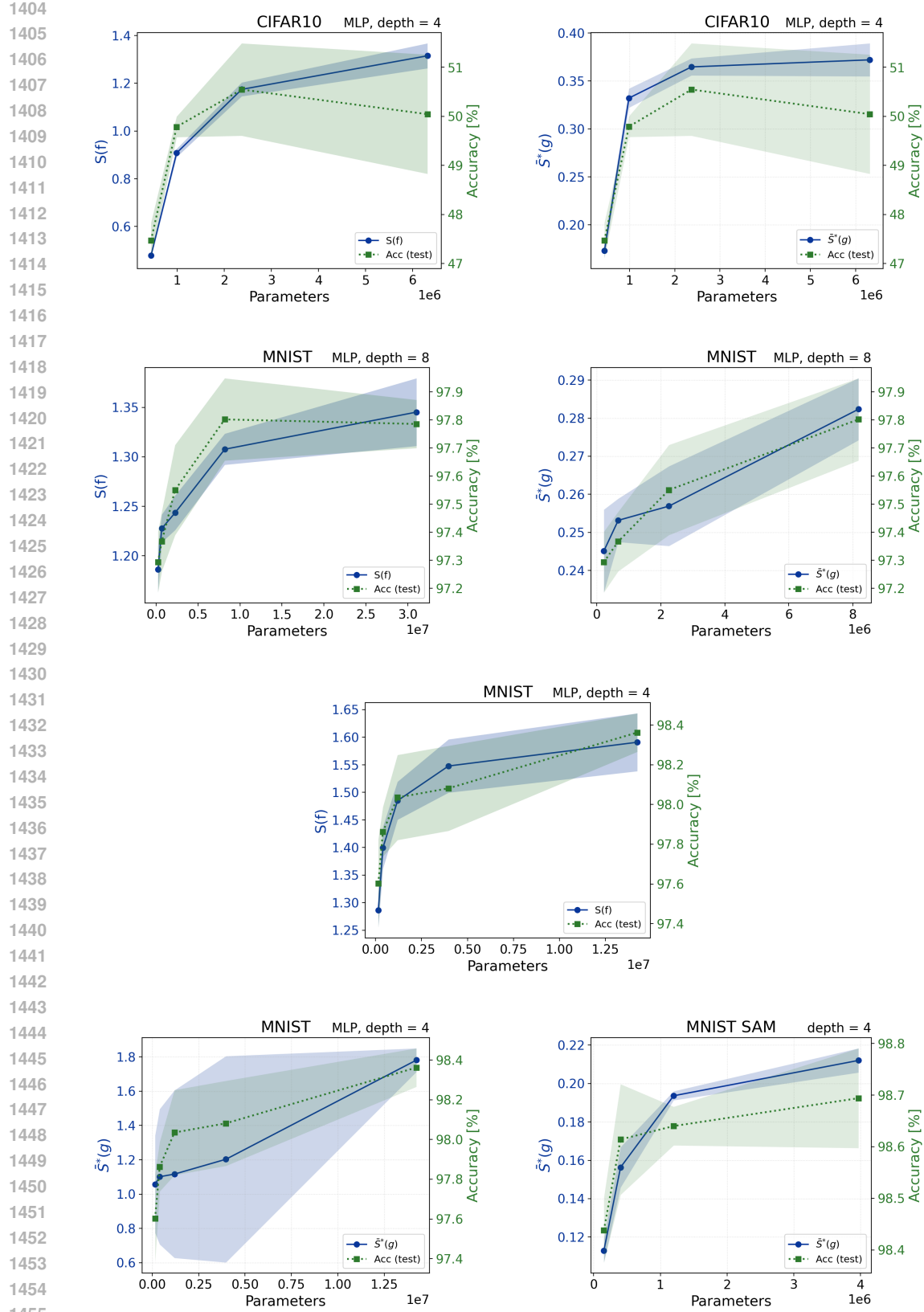
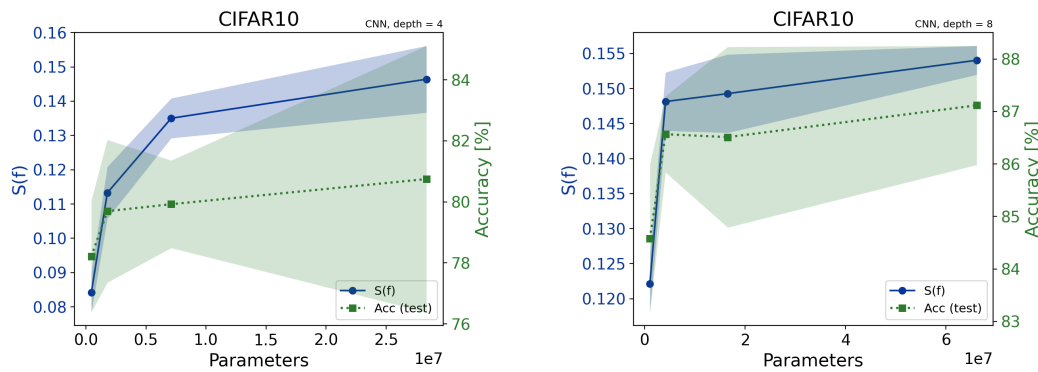
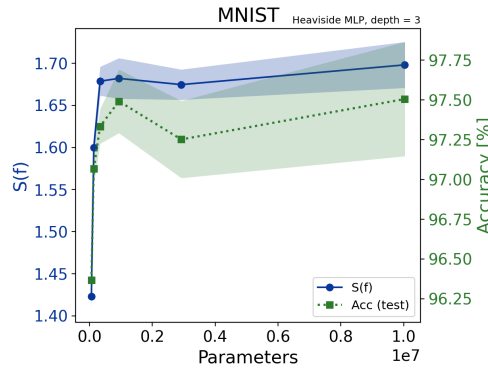


Figure 2: Stability measures for 4- and 8-layer MLPs trained on MNIST and CIFAR-10. For comparison, we also include a 4-layer MLP on MNIST trained with a sharpness-aware optimizer.

1458 **H RESPONSE TO REVIEWERS**  
14591460 **H.1 EXPERIMENTS ON DIFFERENT ARCHITECTURES**  
14611462 Experiments using Vision Transformers are currently still running, but will be added as soon as  
1463 possible.  
14641477 Figure 3: Stability measure for 4- and 8-layer CNNs trained on CIFAR-10.  
14781493 Figure 4: Stability measure for 4-layer heavyside-activation MLP trained on MNIST  
14941495  
1496  
1497  
1498  
1499  
1500  
1501  
1502  
1503  
1504  
1505  
1506  
1507  
1508  
1509  
1510  
1511

1512 H.2 ISOPERIMETRY TEST OF GAUSSIAN TOY-DATA, MNIST AND CIFAR10  
1513  
1514  
15151516 Table 2: Isoperimetry test for Gaussian data with variance = 0.0001,  $c_{\text{true}} = 0.0784$ .

kind	metric	mean	q50	q75	q90
1lip_mlp	$\hat{c}$	0.01462	0.01443	0.01653	0.01892
1lip_mlp	$R^2$	0.9983	0.9985	0.9990	0.9992
linear	$\hat{c}$	0.06701	0.06697	0.06785	0.06836
linear	$R^2$	0.9983	0.9985	0.9990	0.9993
mlp	$\hat{c}$	2.296e+13	2.071e+10	9.311e+11	1.931e+13
mlp	$R^2$	0.9963	0.9965	0.9975	0.9982
trained_margin	$\hat{c}$	3.054	2.957	3.626	4.903
trained_margin	$R^2$	0.9518	0.9497	0.9577	0.9682

1529 Table 3: Isoperimetry test for Gaussian data with variance = 0.001,  $c_{\text{true}} = 0.784$ .

kind	metric	mean	q50	q75	q90
1lip_mlp	$\hat{c}$	0.1113	0.1108	0.1196	0.1303
1lip_mlp	$R^2$	0.9980	0.9982	0.9988	0.9991
linear	$\hat{c}$	0.6701	0.6699	0.6782	0.6839
linear	$R^2$	0.9983	0.9985	0.9989	0.9993
mlp	$\hat{c}$	1.216e+13	2.985e+10	3.281e+11	3.432e+12
mlp	$R^2$	0.9965	0.9965	0.9977	0.9984
trained_margin	$\hat{c}$	15.67	14.41	16.52	25.23
trained_margin	$R^2$	0.9473	0.9477	0.9542	0.9575

1542 Table 4: Isoperimetry test for Gaussian data with variance = 0.005,  $c_{\text{true}} = 3.92$ .

kind	metric	mean	q50	q75	q90
1lip_mlp	$\hat{c}$	0.4963	0.5011	0.5330	0.5556
1lip_mlp	$R^2$	0.9974	0.9977	0.9984	0.9989
linear	$\hat{c}$	3.351	3.350	3.391	3.421
linear	$R^2$	0.9983	0.9984	0.9990	0.9994
mlp	$\hat{c}$	2.826e+12	4.662e+10	8.582e+11	3.753e+12
mlp	$R^2$	0.9968	0.9968	0.9983	0.9988
trained_margin	$\hat{c}$	42.26	35.82	53.31	59.41
trained_margin	$R^2$	0.9548	0.9554	0.9601	0.9628

1555 Table 5: Isoperimetry test for Gaussian data with variance = 0.01,  $c_{\text{true}} = 7.84$ .

kind	metric	mean	q50	q75	q90
1lip_mlp	$\hat{c}$	0.9652	0.9676	1.015	1.065
1lip_mlp	$R^2$	0.9972	0.9974	0.9981	0.9984
linear	$\hat{c}$	6.702	6.712	6.773	6.846
linear	$R^2$	0.9983	0.9985	0.9990	0.9993
mlp	$\hat{c}$	7.927e+16	4.487e+11	2.637e+13	3.904e+14
mlp	$R^2$	0.9968	0.9969	0.9979	0.9984
trained_margin	$\hat{c}$	61.88	56.82	78.33	81.59
trained_margin	$R^2$	0.9598	0.9603	0.9631	0.9677

1566

1567

Table 6: Isoperimetry test for Gaussian data with variance = 0.1,  $c_{\text{true}} = 78.4$ .

kind	metric	mean	q50	q75	q90
1lip_mlp	$\hat{c}$	8.917	8.949	9.408	9.747
1lip_mlp	$R^2$	0.9968	0.9971	0.9980	0.9983
linear	$\hat{c}$	67.12	67.17	67.89	68.62
linear	$R^2$	0.9983	0.9986	0.9990	0.9993
mlp	$\hat{c}$	1.606e+16	6.945e+12	5.642e+13	6.913e+14
mlp	$R^2$	0.9969	0.9970	0.9980	0.9987
trained_margin	$\hat{c}$	240.6	246.0	270.1	276.4
trained_margin	$R^2$	0.9404	0.9434	0.9524	0.9583

1577

1578

1579

Table 7: Isoperimetry results on MNIST: mean and upper quantiles of  $\hat{c}$  and  $R^2$  across models.

kind	metric	mean	q50	q75	q90
1lip_mlp	$\hat{c}$	6.68	6.43	7.20	9.04
1lip_mlp	$R^2$	0.9923	0.9951	0.9970	0.9981
linear	$\hat{c}$	48.02	45.87	56.01	67.69
linear	$R^2$	0.9957	0.9977	0.9991	0.9996
mlp	$\hat{c}$	5.94e+17	2.24e+12	9.37e+13	1.49e+15
mlp	$R^2$	0.9879	0.9896	0.9946	0.9968
trained_margin	$\hat{c}$	973.87	552.88	821.24	2626.08
trained_margin	$R^2$	0.9471	0.9480	0.9563	0.9603

1580

1581

1582

1583

1584

1585

1586

1587

1588

1589

1590

1591

1592

Table 8: Isoperimetry results on CIFAR-10: mean and upper quantiles of  $\hat{c}$  and  $R^2$  across models.

kind	metric	mean	q50	q75	q90
1lip_mlp	$\hat{c}$	28.76	26.08	31.46	39.22
1lip_mlp	$R^2$	0.9817	0.9835	0.9902	0.9943
linear	$\hat{c}$	180.29	165.71	212.00	263.15
linear	$R^2$	0.9931	0.9940	0.9969	0.9989
mlp	$\hat{c}$	3.32e17	1.38e14	2.62e15	5.65e16
mlp	$R^2$	0.9776	0.9798	0.9869	0.9892
trained_margin	$\hat{c}$	4845.16	2247.31	8964.91	11386.31
trained_margin	$R^2$	0.9931	0.9947	0.9979	0.9995

1602

1603

1604

1605

1606

1607

1608

1609

1610

1611

1612

1613

1614

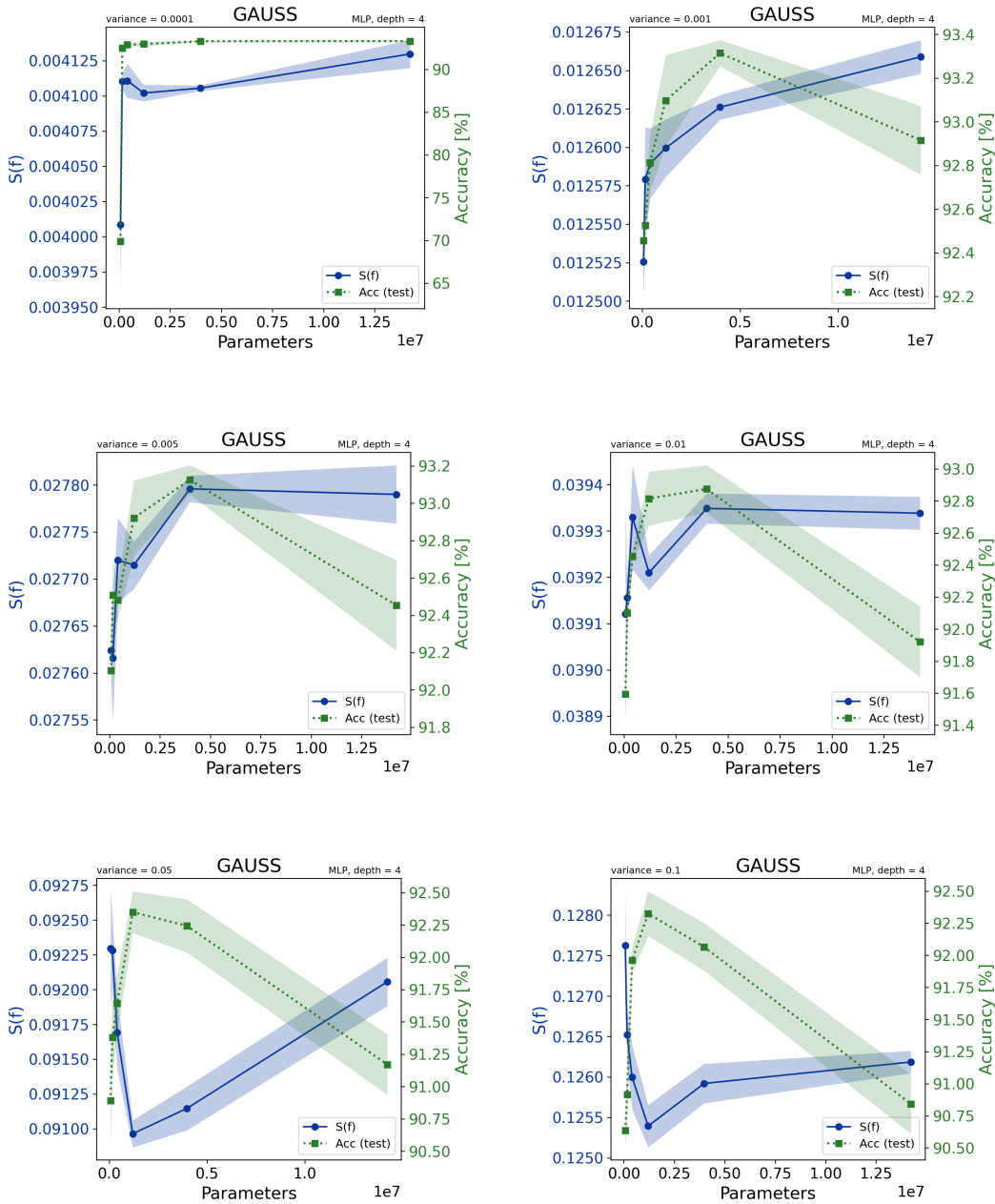
1615

1616

1617

1618

1619

1620  
1621 H.3 STABILITY TEST ON GAUSSIAN DATA  
16221663 Figure 5: Stability measure for 4-layer MLPs trained on Gaussian toy-data with different variances.  
1664  
1665  
1666  
1667  
1668  
1669  
1670  
1671  
1672  
1673